A PRELIMINARY ANALYSIS OF THE DATA FROM EXPERIMENT 77-13 AND FINAL REPORT ON GLASS FINING EXPERIMENTS IN ZERO GRAVITY

W. R. Wilcox
Principal Investigator

R. S. Subramanian, M. Meyyappan
Co-Investigators
Clarkson College, Potsdam, NY

H. D. Smith, D. M. Mattox, D. P. Partlow
Co-Investigators
(W) R&D Center
Pittsburgh, PA 15235

Final Report
Contract No. NAS8-33017

George C. Marshall Space Flight Center
Marshall Space Flight Center, Alabama 35812

Westinghouse R&D Center
1310 Beulah Road
Pittsburgh, Pennsylvania 15235

A PRELIMINARY ANALYSIS OF THE DATA FROM EXPERIMENT 77-13 AND FINAL REPORT ON GLASS FINING EXPERIMENTS IN ZERO GRAVITY

W. R. Wilcox
Principal Investigator

R. S. Subramanian, M. Meyyappan
Co-Investigators
Clarkson College, Potsdam, NY

H. D. Smith, D. M. Mattox, D. P. Partlow
Co-Investigators
(W) R&D Center
Pittsburgh, PA 15235

Final Report
Contract No. NAS8-33017

George C. Marshall Space Flight Center
Marshall Space Flight Center, Alabama 35812

Westinghouse R&D Center
1310 Beulah Road
Pittsburgh, Pennsylvania 15235

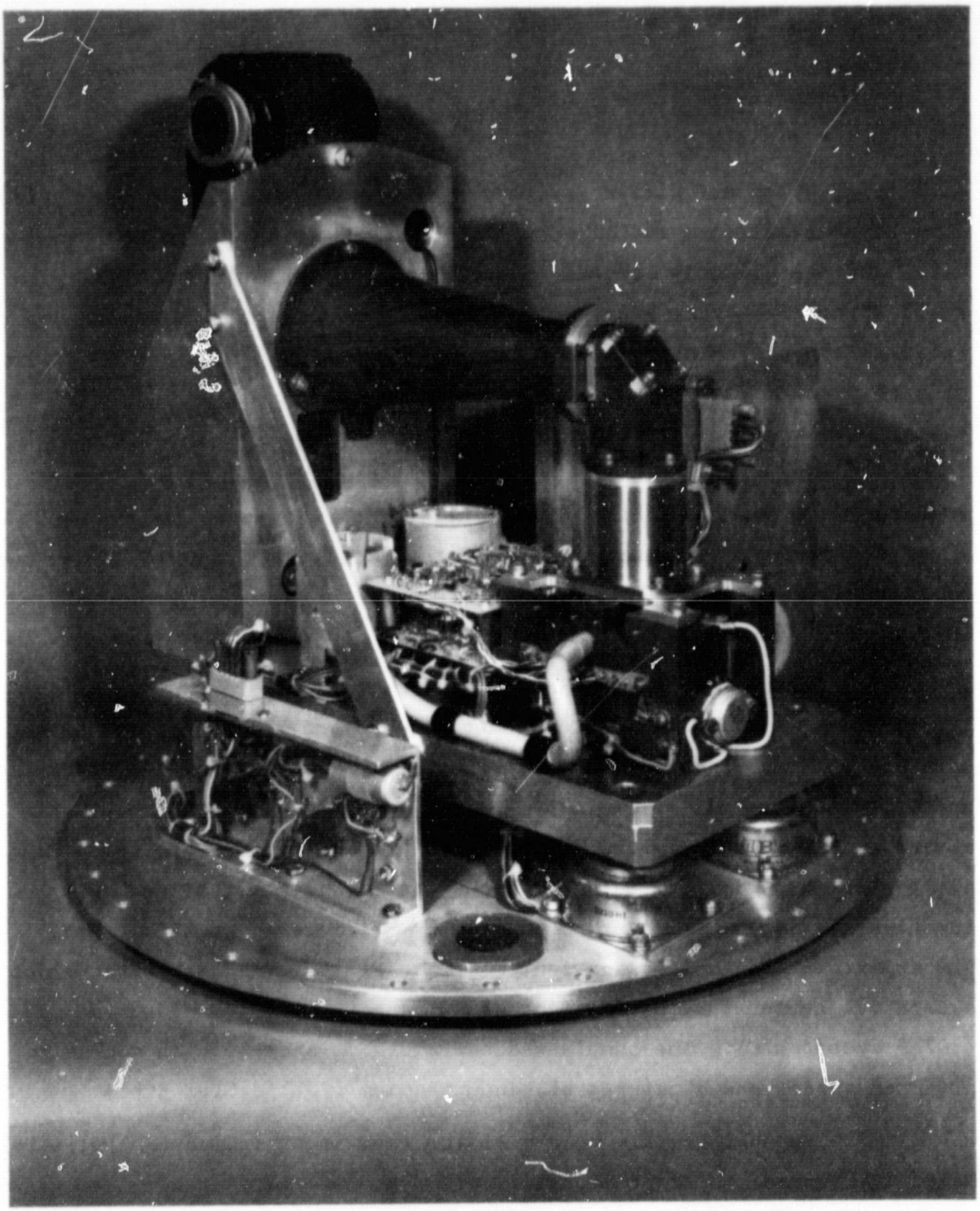

SPAR VIII EXPERIMENT 77-13 FLIGHT APPARATUS

SUMMARY

Bubbles are always formed during glass manufacture. They arise from batch reactions, entrained voids contained in the original batch, etc., and are commonly removed in earth based manufactured glasses by a combination of buoyant and chemical fining procedures. Buoyant fining requires the presence of gravity, and chemical fining requires the addition of a chemical dopant to the glass—neither of which is applicable to containerless melting of ultrapure or special glass systems in space. Thermal fining, i.e. thermal migration of bubbles, on the other hand requires only the imposition of a temperature gradient in the molten glass and does not require physical contact with the sample or the presence of a gravitational field. Theoretical models and ground based experiments both predict the thermal migration of bubbles under reduced gravity conditions.

The objectives of the present study were to demonstrate the thermal migration of bubbles under reduced gravity conditions and if possible provide quantitative data with which to verify current theoretical models. An automatic system was designed to perform an experiment aboard a SPAR rocket payload during the 5-6 minutes of zero gravity available. Experimental data (bubble location and temperatures as a function of time) were recorded on film or telemetered back to earth. The experimental sample was a sodium borate glass (29.9% Na_2O) for which a negative temperature coefficient of surface tension was measured (.0756 dynes/cm°C). The sample was contained in a cell which consisted of fused silica and a tapered platinum rhodium (20%) heater strip.

The photographic record of the experiment indicated that bubbles moved in response to the temperature gradient imposed on the molten glass sample. The motion was both in the plane of the heater strip and perpendicular to it in a way consistent with the temperature gradients measured by thermocouples in the sample. It is not yet known if the data will be quantitative enough to confirm the results of theoretical calculations.

Further work is indicated to modify the experimental apparatus to accept multiple samples and to refine the cell design to orient the thermal gradient parallel to the cell axis. Future experiments should include glasses with positive temperature coefficients, different melting temperatures, and/or borax the glass studied in this experiment over a different temperature range. The effect of impurities, e.g. water, needs to be studied in these systems.

TABLE OF CONTENTS

TABLE OF CONTENTS (Cont'd)

LIST OF FIGURES

LIST OF FIGURES (Cont'd)

1. INTRODUCTION

1.1 Fining

There is one feature common to all aspects of glass melting. At one stage or another, raw materials are melted together. This liberates gases which were chemically combined or adsorbed on the raw material, leading to bubble entrapment. To render the glass transparent and to provide useable strength levels, these bubbles are eliminated in a process known as "fining". While this particular terminology is limited to bulk glasses, the requirement for eliminating bubbles is a dominant feature of the processing of most glass-containing systems. Ceramic-to-metal seals (high pressure sodium lamps) and glass-to-glass or glass-to-ceramic seals (cathode ray tubes) are formed with powdered glass (solder) seals. Hermeticity and acceptable strength directly correlate with the elimination of the void structure. Predictability and reliability in integrated circuits are commonly ensured by the use of passivating glass coatings. These are applied by elaborate techniques using powdered glass in liquid slurries to assure thin continuous coatings. The typical low expansion semiconducting materials require glasses which barely fuse at temperatures close to the stability limits of some of the components. The necessity of eliminating the entrapped bubbles dictates the times required at these elevated temperatures.

Another example of glass processing which is regulated by bubble behavior is conventional porcelain enameling. In this process, bubbles must be eliminated to the point of leaving a smooth glass surface, but in this particular application a rather well defined subsurface bubble structure imparts desirable performance benefits. In fact, certain additives, such as clay, are introduced to generate a bubble structure. The prevention of the defect called "fishscale" in sheet iron is one such benefit.

1.1.1 Buoyant Fining

In spite of the great wealth of experience possessed by glass manufacturers, little is understood about the process of fining and even less is understood about bubble elimination in sealing glasses or enamels. The traditional viewpoint[1-2] of glass fining is based on the effect of additives, called "fining agents." These decompose rapidly, to form new bubbles, or the gases diffuse into existing bubbles, causing them to grow, whereupon they rise quickly out of the melt under the action of buoyant forces. The velocity at which bubbles rise in the molten glass may be approximated by the following equation:

$$V = \frac{D^2 g \rho}{12\eta} \qquad (1)$$

where D = bubble diameter
g = gravitational constant
ρ = density of the melt
η = viscosity of the glass.

Simple calculation shows that beneath a particular size bubble, buoyant fining does not occur fast enough to eliminate bubbles in the times used in conventional processing. For example, a bubble 0.1 mm in diameter in a lime glass with a viscosity of 100 p will rise about 17 cm/day - too slow for commercial processing. An additional mechanism is necessary to explain the fining of commercial glasses.

1.1.2 "Chemical Fining"

Another important mechanism of fining of commercial glasses is due to small amounts of chemical agents added to the batch. Traditionally, arsenic and antimony oxides as well as sodium sulfate have been employed for this purpose in concentrations less than 1 weight percent of the batch. The role played by chemical agents is not quite clear at this time. Two schools of thought prevail, both supported by incomplete experimental evidence. The experiments of Greene and Gaffney[4] as well as others (Cable et al.[5]) suggest that bubbles dissolve more rapidly

the presence of fining agents than in their absence. This may be attributed to chemical reactions of the diffusing gas with the fining agents. However, Nemec[6] has recently observed that bubbles, in fact, grow more rapidly in the presence of fining agents than in their absence. Since the buoyant rise velocity is proportional to the square of the bubble diameter, his argument is that fining agents promote the growth and therefore rapid rise of small bubbles from the melt. The reason for this confusion in the literature and the two opposing schools is simply that the experiments were not performed under sufficiently controlled conditions. The initial gas concentrations in the melt which are crucial in determining whether the melt is undersaturated or supersaturated with respect to a given gaseous species were not controlled in the different experiments to a sufficient degree. Furthermore, the melts typically contained several dissolved gaseous species. Therefore, even if a single-component bubble is injected, soon, it would become a multicomponent bubble with some species possibly diffusing in while the others are diffusing out, and complex reactions would be simultaneously occurring in the melt. Thus, while chemical fining is effective as an industrial practice, much remains to be done in elucidating the actual mechanisms by which it occurs.

1.1.3 "Thermal" Fining

"Thermal" fining, to coin a parallel phrase, is a mechanism that has been largely overlooked and little understood.[7] A temperature gradient, with its effect on surface tension, produces a displacive force on bubbles. Thermal fining may be the principal mechanism of bubble elimination in sealing, soldering, and enamelling operations. It is commonly observed that bubbles quickly come to the surface of glass enamel, regardless of the orientation of the enamel. Since seals, solders, and enamels are typically heated externally, it is presumed that a driving force toward the external surface is established on the bubbles in the fluid glass.

While significant evidence has been reported[8-12] which confirms that gas bubbles can move in a temperature gradient, no evidence has been reported for this phenomenon in glass systems, in spite of its obvious importance in glass sealing and enamelling. The effect of this mechanism has possibly been observed in experiences with direct electric melting of bulk glasses. Contrary to fuel fired furnaces, electric melters are hottest at the bottom of the tank. This gradient would oppose buoyant fining, and indeed, electrically melted glasses require more time to fine, although there are other factors which contribute to this.

While the mechanism of thermal fining is obviously of great commercial significance in many high technology applications, it represents an even more important mechanism in the space processing of glasses. There has been considerable interest in producing glasses in a zero gravity environment, particularly because the materials could be cooled in a containerless fashion avoiding heterogeneous nucleation as well as contamination by the container walls. It has been proposed that certain difficult glass formers be produced in free fall for this reason (M. C. Weinberg, "Glass Processing in Space", Glass Industry, p. 22, March 1978, G. F. Nielson and M. C. Weinberg, "Outer Space Formation of a Laser Host Glass", J. Non-Crystalline Solids, 23, 43, 1977). One of us (RSS) is currently involved in planning space shuttle experiments on the use of thermal gradients for fining bubbles from levitated molten glass drops (see R. S. Subramanian and R. Cole, "Experiment Requirements and Implementation Plan (ERIP) for Physical Phenomena in Containerless Glass Processing", Marshall Space Flight Center Document 77FR010, August 1979).

1.2 Thermal Fining in Molten Borax: Ground Based Laboratory Results From Demonstration Study

As reported earlier[13], ground based experiments were run to demonstrate bubble movement and the feasibility of the techniques to be employed for a SPAR experiment. Thermal migration of bubbles in

molten borax was observed in both a quartz capillary tube and in an inverted silica channel. The temperature gradient was generated by passing electrical current through a tapered platinum strip under the capillary tube or channel. The best observations were made with the inverted channel because its shallow depth (500 μm) allowed all bubbles to be seen at once and because there was good thermal contact of the melt with the heating strip.

This demonstration experiment was run by melting a piece of glass cane containing bubbles into an inverted channel in a fused silica cover using the platinum heater strip. A simple schematic of this cell is shown in Figure 1.2-1. During the first minute or so the molten glass flowed into the channel and formed a thin film between the silica cover and the platinum heater strip. Once the channel was full and the thin film occupied the rest of the areas between the silica cover and platinum strip, the physical flow of the melt ceased. This was clear from the fact that the physical boundaries did not change position and bubble groups no longer moved *en masse*. During that initial melt down period many of the bubbles moved toward the hot spot and coalesced into few larger bubbles. However, bubbles further away from the hot spot did not have time to move far during that time and they continued to move individually toward the hot spot after the glass itself ceased flowing. At this point several photographic sequences were taken with time intervals of 5 or 10 seconds in the sections with rapidly moving bubbles, and 20 seconds in the outer region with slower moving bubbles.

The bubble migration observed is illustrated by Figure 1.2-2. Here bubbles next to the channel wall (dark band just above two larger bubbles) are shown migrating toward a region of higher temperature. Two features to look for in this series of pictures are: (1) bubbles accelerate as they move to higher temperature, and (2) larger bubbles move faster than smaller ones. The difference in velocity due to size is illustrated by the second largest bubble overtaking the smaller one just ahead (to the right) of it by the 20-second frame. Most interesting was an apparent attraction of bubbles to one another, enhancing coalescence. This phenomena had not been reported before, and stimulated enthusiasm for a flight experiment.

Dwg. 7745A27

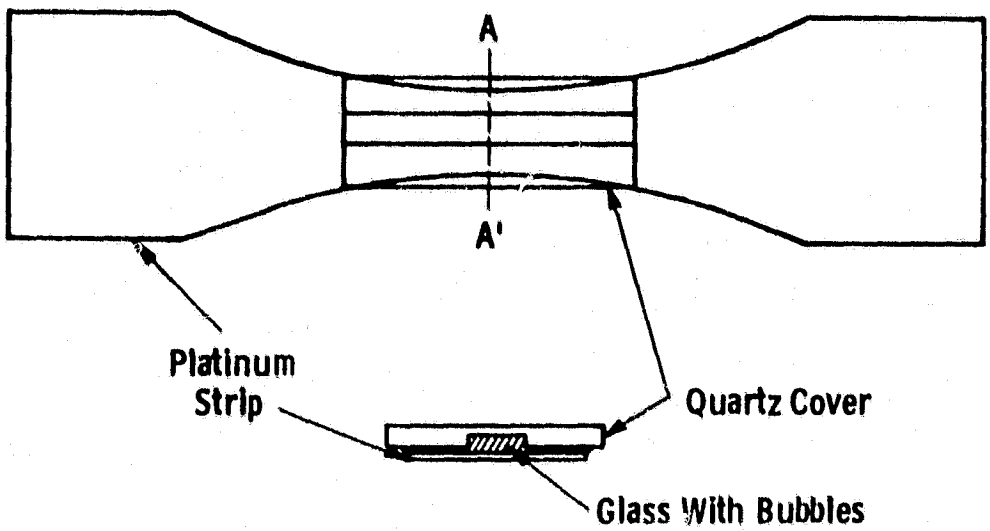

Fig. 1. 2-1—Quartz cover with inverted channel in place on platinum heater strip

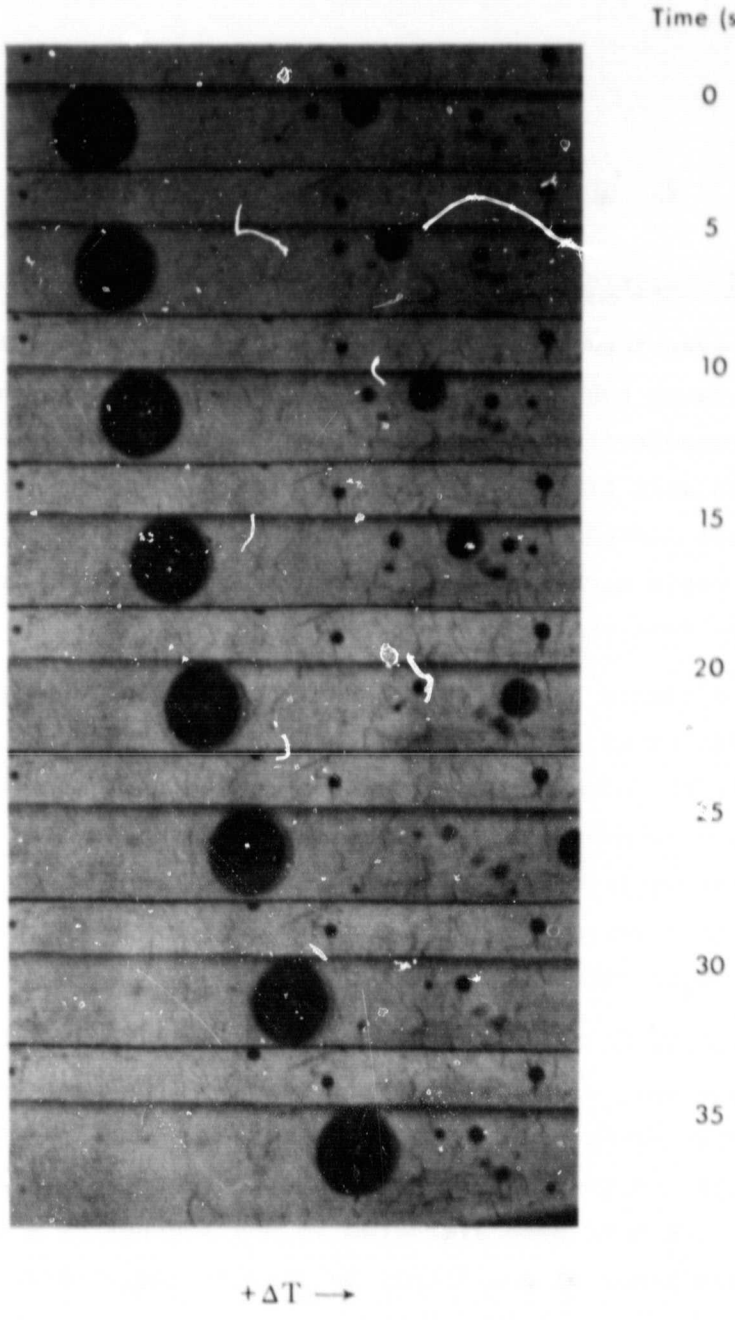

Figure 1.2-2 - Bubble migration in molten borax. Large bubble is 260 μm in diameter. Wall of channel in which bubble moves just above large bubble. Small bubbles at top of each frame are trapped between platinum heater strip and silica cover and do not move. (Ground based demonstration experiment.)

2. GLASS FINING IN ZERO GRAVITY PROGRAM

2.1 Need and Justification for Low-G Experiments

As described above, we demonstrated that a temperature gradient can cause bubbles to move in a temperature gradient. However, for several reasons it was impossible to do glass fining experiments on earth which were free of the effects of gravity. Most obvious is buoyancy, which can cause bubbles to rise, and natural convection, leading to a rapid global movement of the glass melt and irregular thermal losses from the apparatus.

If a single bubble were used in a vertical apparatus, then bubble movement rates could be measured. However, because of buoyancy of the bubble, the movement rate would be quite different than in space. Nevertheless, such ground-based experiments have been used to test approximate theoretical results. For example, Young et al. adjusted the temperature gradient so as to exactly compensate for buoyancy, i.e., the movement rate was zero.

In glass fining we have the added complication that many bubbles are present, with a variety of sizes. Thus with gravity they will all rise at different rates, with the large ones overtaking the small ones. In addition, as we have observed experimentally, the bubbles appear to have been attracted to one another in a temperature gradient. Such behavior could only be studied unequivocally in space.

2.2 Objectives

Ground based studies have shown that bubbles in molten sodium borate (borax) do move in response to an imposed temperature gradient. It was the primary objective of the experimental part of this study to demonstrate that this observed movement was not due in some way to

gravitational influences. The minimum success requirements to meet this objective were designated as follows:

1. A good photographic record of the motion of bubbles in molten sodium borate covering a period of at least 60 seconds at zero gravity.
2. A hot spot temperature of about 900°C.
3. A temperature gradient of several hundred degrees per centimeter in the molten glass region photographed.

It was also hoped that the thermal region of the hot stage would be known well enough so that the experimentally measured motion could be compared meaningfully with theory also to be generated as part of this program. The photographs should also have provided valuable information about bubble-bubble interactions and bubble-wall interactions.

Parallel with the experimental work, there was the need to advance the quality of the current theoretical models for bubble motion due to the presence of a temperature gradient. This modeling was to more accurately solve the hydrodynamic equations that govern bubble motion, and to extend the theory to bubble-bubble and bubble-wall interactions.

To make the comparison between theory and experiment as meaningful as possible, the important physical parameters, viscosity and surface tension, needed to be known as accurately as possible. Therefore, measurements of the surface tension were made as a function of temperature on a melt of known composition. Suitable viscosity data were identified in the literature, so it was not necessary to perform these measurements in the laboratory.

2.3 Program Task Definition

This program was organized into four tasks:

2.3.1 Task I

Develop, assemble, and qualify a piece of experimental hardware that could perform the experiment automatically and record photographically and telemetrically all of the critical experimental results. This included the manufacture of the experimental sample for the flight. The Westinghouse R&D Center carried out this task.

2.3.2 Task II

Make very accurate measurements of the surface tension of dry, molten sodium borate under a dry N_2 atmosphere as a function of temperature. The temperatures included the total range to occur in the experiment. The Westinghouse R&D Center carried out this task and published the results in the Journal of Physics and Chemistry of Glasses, Vol. 21, No. 6, Dec. 1980, pp. 221-223.

2.3.3 Task III

Develop mathematical models for bubble motion and interaction. This included the development of computer programs which could make the necessary calculations. These studies were made by Clarkson College of Technology. Two articles based on this work have been accepted for publication and will shortly appear in the Journal of Colloid and Interface Science and the AIChE Journal (21,22). A third article is currently under preparation.

2.3.4 Task IV

Evaluate bubble behavior from photographic record of SPAR experiment, using motion analyzer at Clarkson College of Technology. Compare with theoretical predictions. An article based on this work is currently under preparation.

3. EXPERIMENT APPARATUS FOR THE SPAR VIII FLIGHT

The entire experiment was designed to be packaged in a 17" x 24" sealed cylindrical canister. The AFT plate of the canister was blind tapped formounting 4 shock pads which supported the critical sections of the experiment. These sections were: 1) the camera, 2) microscope tube, 3) experiment hot stage, 4) stage support heat sink, 5) the electronic circuit boards for heater power control and thermocouple amplifiers.

A printed circuit card cage and some other sundry electrical components were hard mounted directly on the AFT plate. In the following sections, more detail is provided on the Photographic System, which consisted of the camera and microscope tube with objective lens, Experimental Hot Stage and the Electrical System.

3.1 Photographic System

The layout of the photographic system is shown in Figure 3.1-1. The system consisted of an objective lens, phototube with front surface mirror to deflect the optical path 90°, camera without lens and two light pipes that acted as edge illuminators. One light pipe was actually used with the other serving as a backup.

The camera was a Nikon F-2 equipped with a 250 frame magazine back and a Nikon MD-2 motor drive. The camera was actuated by an external timing circuit. The current drawn by the camera motor-drive was monitored by telemetry and served as a record of the actual photographing rate.

The objective lens was a 1.2X Nikon microscope objective which provided ∿6X magnification. This lens had the necessary depth of focus and included enough surrounding detail to make orientation and scaling

Dwg. 7745A29

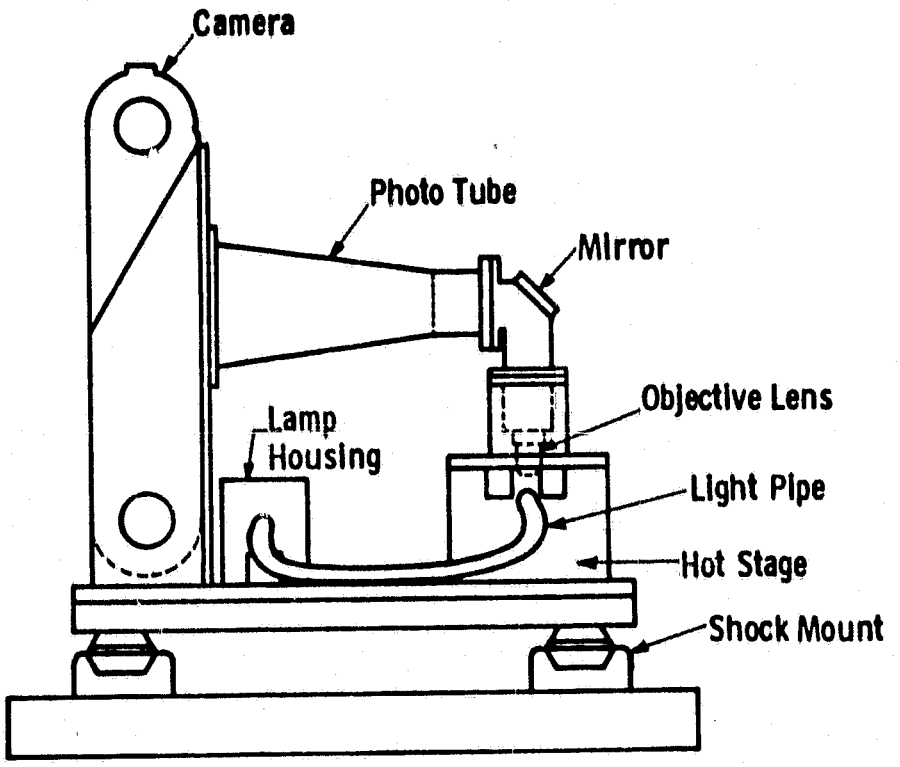

Fig. 3.1-1—Major components of the photographic system

of the photographic record relatively straightforward with little chance of serious error. The magnification was still good enough to track ~10 μm bubbles.

3.2 Experiment Hot Stage

An exploded view of the hot stage and of the sample plate-heat shield assembly is shown in Figures 3.2.1 and 3.2.2. The hot stage was designed to perform the following functions:

- To hold the sample plate-heater strip with accompanying heat shields in alignment with the objective lens so that the cell could be properly photographed.
- To allow power to be applied to the heater strip to establish the experimental conditions and light to be ducted to the glass sample to properly illuminate it.
- To act as a sink for the heat generated by the heater-strip.

The heat shields and sample plate were fused silica. The heat shields were gold flashed on the side away from the sample plate only, to reduce the chance of shorting the thermocouple leads. The spacers or shims isolating the plate and shields were made from either Kapton tape or silicone rubber. The entire stack is shown in more detail in Figure 3.2-2. This stack was pre-assembled so that with minimal alignment it could be automatically located on the optic axis and in the focal plane of the photographic system. The thermocouple leads were arranged to coincide with the correct terminal on the side of the hot stage. These leads were captured by laminating them between pieces of Kapton tape which also insulated them from the hot stage and thermocouple clamp.

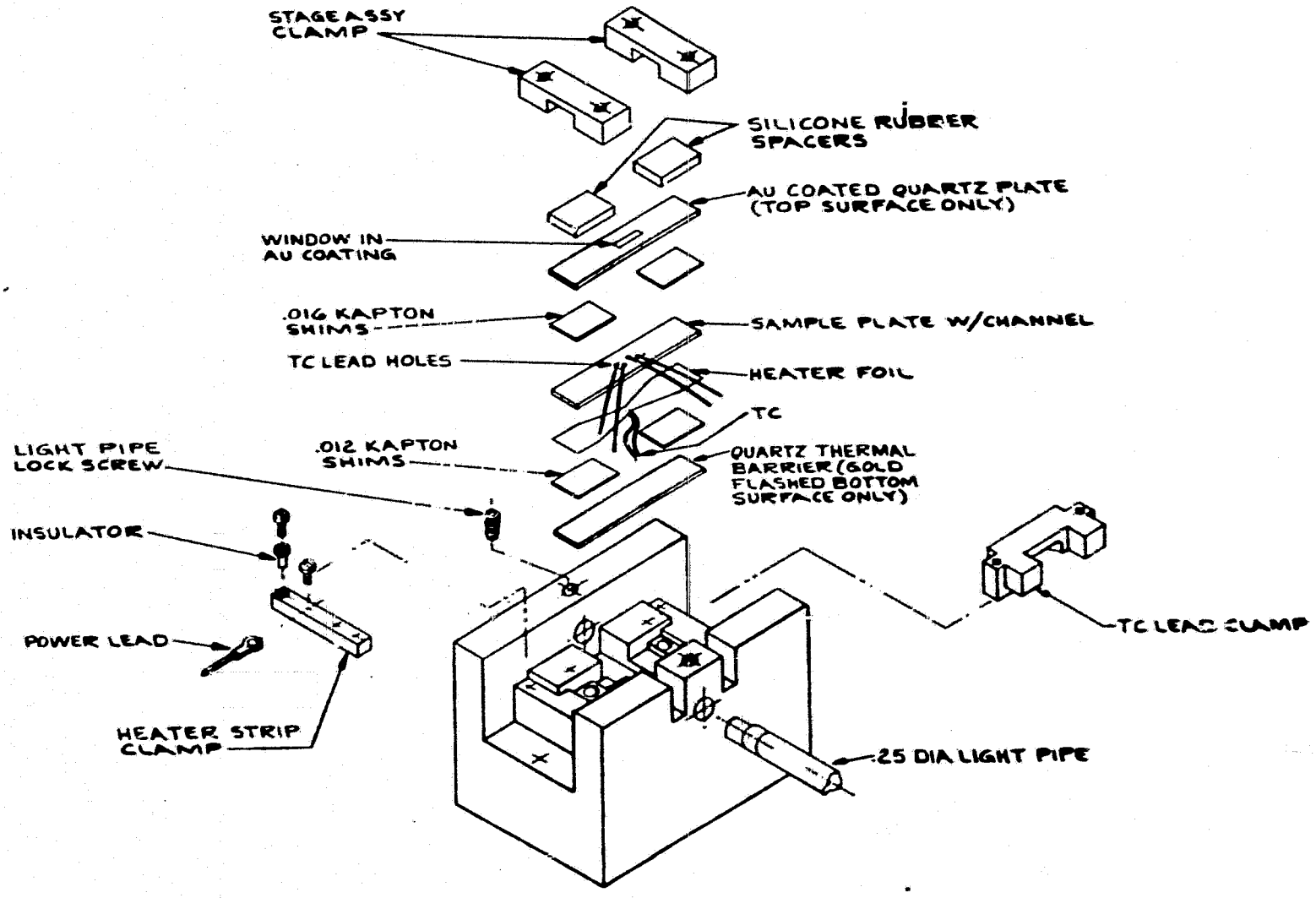

Figure 3.2-1 - Experiment hot stage composite assembly.

Dwg. 7741A35

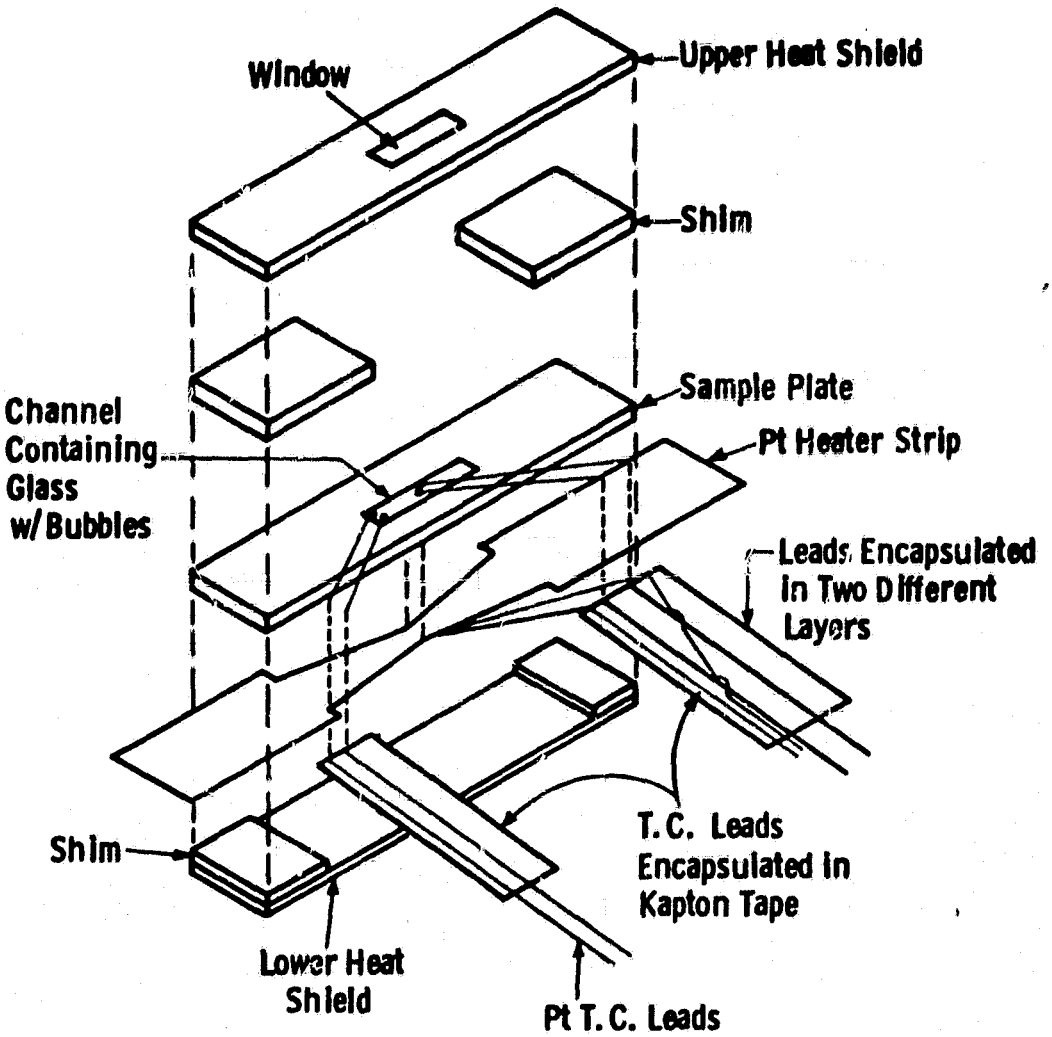

Fig. 3.2.2—Expanded schematic of sample cell assembly

Two thermocouples were implanted in the glass with the leads exiting from the top of the sample plate through .015" holes. The other thermocouple was spot welded to the bottom of the platinum-rhodium heating strip at the hot spot. This latter thermocouple was used to control the strip temperature while the first two monitored the temperature and the temperature gradient in the molten glass.

3.3 Electrical Control System

The electrical control system for this experiment consisted of the five primary functional blocks shown in the block diagram of Figure 3.3-1. These functional blocks are: (1) isolating power supply, (2) logic circuitry, (3) power conditioning circuitry, (4) signal conditioning circuitry, and (5) the experiment itself. The relative relationships of these functions are indicated in the block diagram. Primary power to the system was derived from the 28V dc bus. Power for the isolating power supply, logic circuitry, and power conditioning circuitry was derived directly from this bus. The signal conditioning circuitry for amplifying the thermocouple signals and generating telemetry signals was isolated ohmically from the 28V dc bus. This isolation was maintained by transformer isolation of power signals and light-coupled (LED) isolation of control signals.

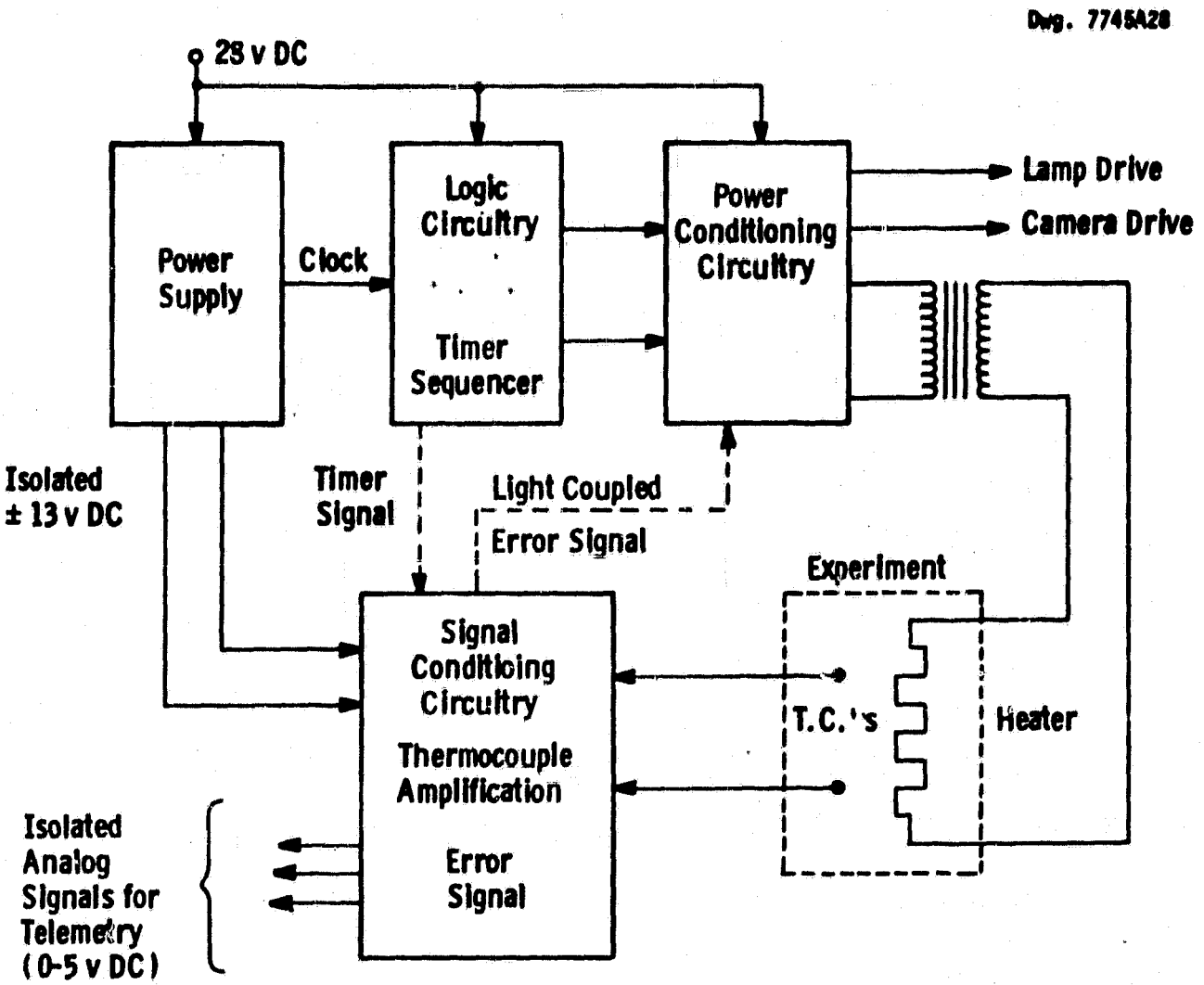

Fig. 3.3-1—Block diagram of the control system

3.4 Temperature vs. Position and Time in Typical Flight Samples

The first objective of the experimental apparatus was to develop a stable temperature gradient in the sample of glass containing bubbles. The gradient was generated by the tapered platinum rhodium (20%) heater strip. The gradient was oriented along the axis of the strip pointing horizontally toward the narrow spot where the hot spot occurred and vertically into the strip (because a large vertical gradient also existed).

3.4.1 Temperature vs. Position

The platinum (rhodium 20%) heater strip shown in Figure 3.2.2 was cut from .001" x .4" (10 mm) strip with a rubber die. The tapered section of the strip decreased in width from 6 mm at the ends to 2.5 mm at the center. This took place over a distance of 10 mm.

The temperature profile of several heating strip-sample assemblies was determined using an IRCON model #300 T5C optical pyrometer. This model read the radiation in the interval 2.0 - 2.6 μm. The spot size read was 2 mm in diameter.

The following procedure was used to determine the temperature profile. The central hot spot was read with the IRCON and the emittance control adjusted until the pyrometer read the same as the thermocouple on the heater strip. The stage was then moved in .625 mm increments and a temperature measurement made for each increment. The pyrometer was kept stationary. Representative results are shown in Fig. 3.4.1-1.

The results are summarized as follows:

- The temperature gradient measured in this way was linear over the region to be photographed.
- The gradient shape was quite reproducible from strip to strip.
- The gradient increased with temperature from ∿300°C/cm when the hot spot read 700°C to ∿550°C/cm when the hot spot read 1035°C.

Curve 728466-A

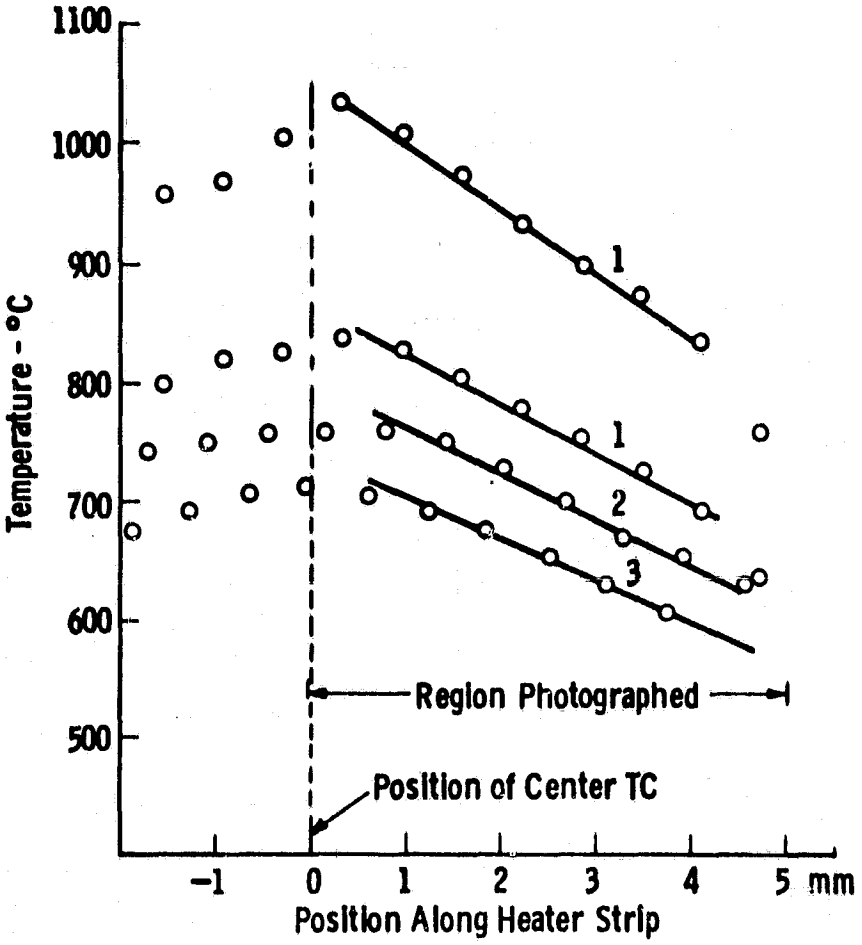

Fig. 3.4.1-1—Some typical temperature profiles measured on the hot strip heater with the IRCON. The readings were made on a complete hot stage assembly without the upper heat shield. Results from three separate strips are shown. The lines are a visual fit to the points

Temperatures measured by the control thermocouple on the bottom of the platinum heater strip and by another thermocouple at the top of the channel directly above it in the glass indicated a strong vertical gradient in all of the sample plate assemblies. The addition of the gold-flashed heat shields decreased its magnitude about 20%. With a shield, gradients of between 26°C and 50°C were measured. A best estimate would be 30-40°C because the presence of large bubbles in some cases appeared to raise the measured gradient.

3.4.2 Temperature vs. Time

The time-temperature characteristics of several sample plate assemblies were recorded during test runs while the electronic control system was adjusted. Figure 3.4.2-1 shows a typical set of traces from the thermocouples in the glass. A final horizontal gradient of 310°C/cm was generated in the case shown. It was very important to accurately locate the vertical position of the thermocouples after the flight experiment because of the vertical gradient.

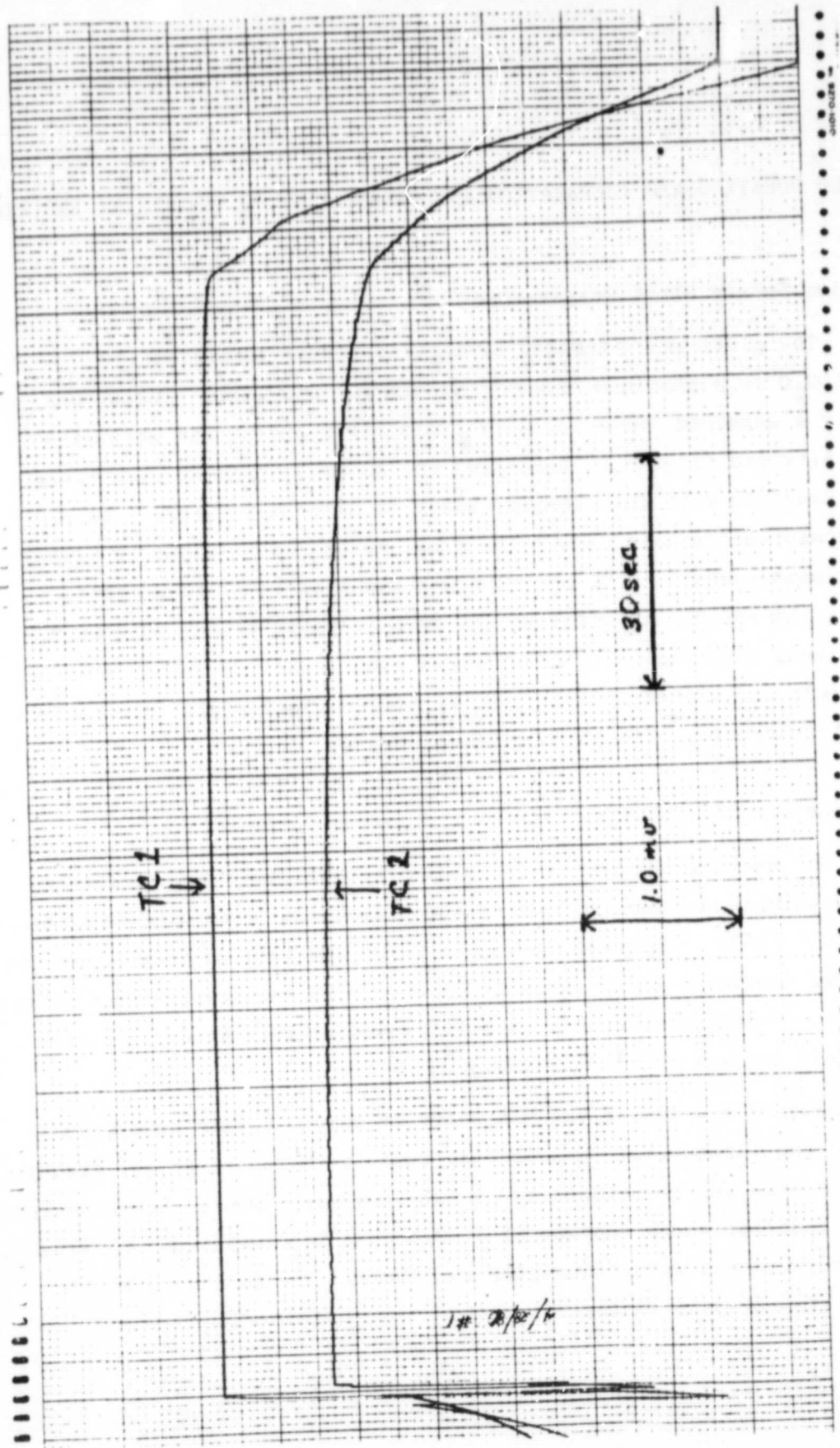

Figure 3.4.2-1 - Time-temperature profile for a sample plate assembly in place in the hot stage. TC1 indicated a maximum temperature of 887°C and TC2 a maximum temperature of 732°C.

4. SODIUM BORATE GLASS PREPARATION AND FABRICATION OF THE FLIGHT EXPERIMENT CELL

4.1 Sodium Borate Glass Preparation

The glass was prepared by melting Fisher certified $Na_2B_4O_7 \cdot 10H_2O$ in a platinum crucible at 800°C. The water content was reduced to a measured (BOH) value of .0234% by bubbling the melt with very dry nitrogen (liquid N_2 boil-off) for 17 hrs. Samples were taken from the crucible melt for chemical analysis before and after surface tension measurements were made. Na_2O was found to be about 1% higher after the measurements. Since Na_2O was expected to preferentially volatilize, the before and after values were averaged giving 29.9 wt % Na_2O. At this point one millimeter glass cane (rod) was drawn from the crucible melt and stored under dry N_2 in sealed glass vials in anticipation of constructing flight experiment samples.

4.2 Surface Tension and Viscosity of the Sodium Borate Glass

The surface tension of the sodium borate glass was carefully determined using a maximum pull-on cylinder technique over the temperature range 725°C - 925°C. The data over that range are well reproduced by the equation σ(dynes/cm) = 261 - .0756 T(°C), where the temperature coefficient -.0756 has the units dynes/cm-°C. A full report of this study is given in the report by Partlow et al. (1980)[14].

Several studies of the viscosity of sodium borate have been reported in the literature. However the study by Matusita et al. (1980)[15] specifically measured the viscosity of very low water sodium borate melts. They state that the water content of a 29.6 wt % Na_2O melt was .03 mole %, which is close to the value found for our glass. The following values were taken from a graph in their report:

700°C - 681 poise

800°C - 40 poise

900°C - 5.0 poise

The other studies, by Shartsis et al. (1953)[16] and Kaiura and Toguri (1976)[17], were performed on glass melts that probably contained more water, although their results do not differ greatly from the above values.

4.3 Fabrication of the Flight Experiment Cell

The flight sample was encapsulated by a fused silica plate 1 x 12 x 48 millimeters in dimensions. The sample cavity itself had the dimensions .5 x 1 x 10 millimeters (see Figure 4.3-1). The sixth surface of the sample was enclosed by the platinum heater strip. The elimination of all free surfaces was necessary to prevent thermocapillary convection from occurring and generating bulk flow in the melt. The fused silica slide was also an excellent optical medium to photograph through. The only drawback of this construction was the generation of small cracks in the fused silica wall bounding the sodium borate glass. However, as seen below this was an unavoidable condition.

The flight experiment sample was generated in two steps. First the leads of two platinum-rhodium thermocouples were threaded through the ports in the top of the sample chamber and then a suitable piece of glass cane (∿1 cm long) was laid in the channel on top of the thermocouple beads. The system was placed in a furnace at ∿1000°C for ∿45 seconds. The furnace was constantly flushed with dry N_2 and the cooling sample was flushed with N_2 also. Figure 4.3-1 a b shows the sample plate before and after the first firing. In the second step, the platinum rhodium 20% heating strip was attached to the sample plate by fusing the sodium borate glass through passage of current through the heater strip itself. When fused by the platinum strip, the glass flowed into an equilibrium mechanical configuration under the influence

of capillary and gravitational forces. By including this step, an experimental cell was produced in which the glass had completely filled the inverted channel and also filled the thin space between the silica cover and the heater strip. This physical distribution of glass was similar to that observed previously in the demonstration study. Hence, it was expected that very little bulk flow would occur during the initial phase of the flight experiment because most if not all of the bulk flow occurred during the fabrication step. Incidentally, during this step any bubbles present were observed to migrate toward the hot spot. Figure 4.3-1 illustrates the effect of this second firing. Again a stream of dry N_2 was directed over the sample during this procedure. The sample was stored under dry N_2 until incorporated in the sample cell assembly described previously.

The cracks in the sample glass caused by the expansion mismatch between the sodium borate and the fused silica plate acted as bubble generators for the experiment. Bubbles put into the glass prior to the final firing were almost always completely removed by subsequent processing due to thermocapillary movement. The cracks produced microvolumes which were filled with the dry N_2 atmosphere in which the sample was stored. These voids rounded off into spherical bubbles during the melt down of the glass at the beginning of the experiment. By forming many bubbles, their distribution throughout the glass assured that several would be in a position to provide useful data.

A complete sample cell assembly is shown in Figure 4.3-2. This assembly was constructed so that the glass sample was in the focal plane of the photographic system as installed and so that the thermocouple leads were captured for much of their length, preventing any chance of shorting.

One final comment about the fabrication of the flight experiment cell. Though the fabrication steps seemed straight forward, there were several processes occurring that were difficult to control. These included the wetting of the silica and platinum surfaces and flow of

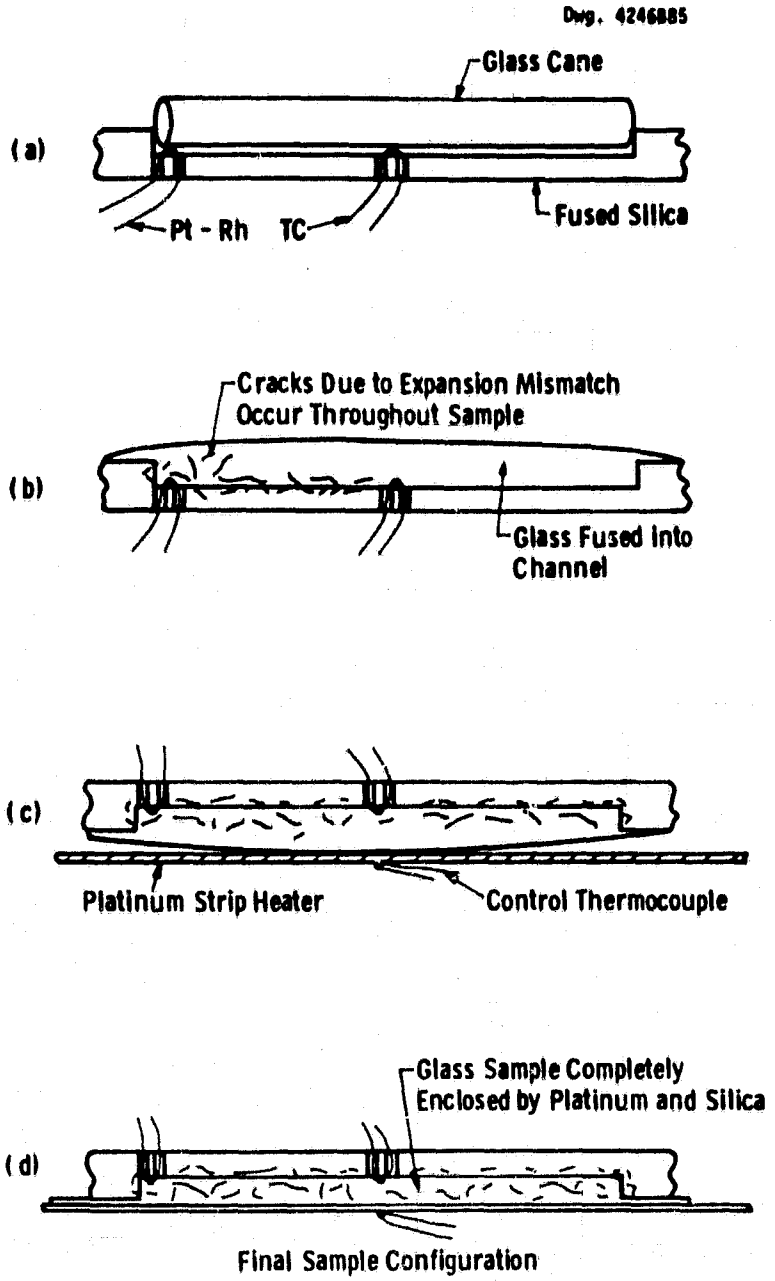

Fig. 4.3-1—a) and b) First step in assembling the flight sample. The glass (Na borate) was fused filling the channel and encapsulating the thermocouples. Second step.c) and d). The platinum heater strip was used to fuse the sample glass which flowed to bring the system into mechanical equilibrium. Crazing (formation of small cracks) occurred throughout the glass and in the surrounding silica plate. The channel was 0.5 mm deep.

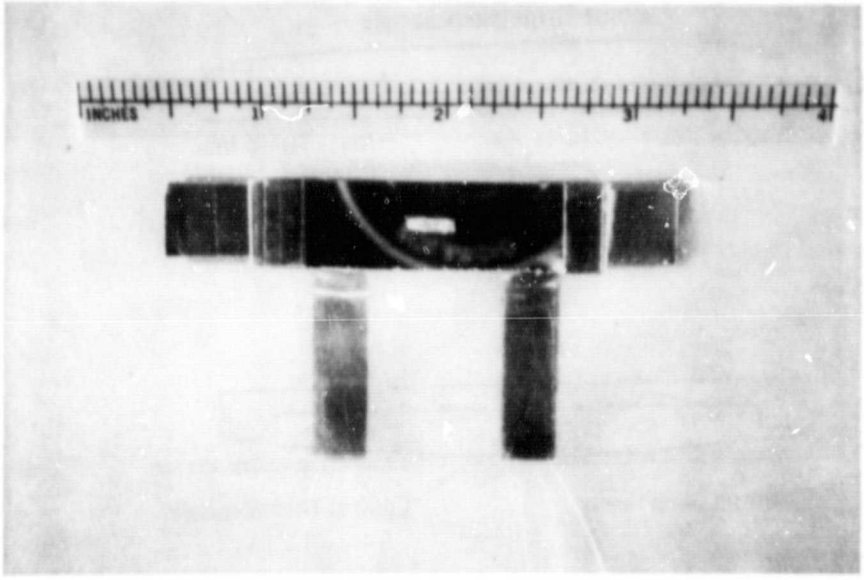

Figure 4.3-2. Top view of complete sample cell assembly ready for installation. Figure 3.2-2 shows the expanded schematic of the assembly.

the melted glass, the formation and migration of bubbles during the second melting step, and the cracking process that degraded the photo-optics but generated bubbles for the experiment. As a result of these factors, the yield of good cells varied from 10 to 50 percent.

5. THEORY

Young, Goldstein and Block[8] (YGB) were the first to consider bubble motion in a surface tension gradient. They assumed a spherical bubble and neglected convective momentum and heat transfer. That is, they solved the creeping flow hydrodynamic equations and the conductive heat transfer equations. In the absence of gravity they predicted a bubble movement velocity V of

$$V = \frac{\partial T}{\partial x} \frac{\partial \sigma}{\partial T} \frac{a}{2\eta} \qquad (1)$$

where T is temperature far from the bubble, x is distance along the temperature gradient, σ is surface tension, a is bubble radius, and η is viscosity. The results of YGB have been verified experimentally for low viscosity fluids in relatively low temperature gradients[8,18-20].

Molten glasses have high viscosities, and some processing requirements may call for moderately high temperature gradients. Under such conditions the movement rate may be sufficiently low that the creeping flow approximation is still valid, but appreciable convective heat transfer may occur. Convective heat transfer would lower the temperature gradient along the bubble surface, and thereby lower the movement rate V.

5.1 Single Bubble in Large Melt

We first attempted to develop a general finite difference numerical scheme for the single bubble problem, using an M.S. student, Vincent Milito, who was not actually paid from this contract. Several cases at low Marangoni number* were solved. Better agreement with the experiments of Hardy[18] was obtained than provided by YGB's results. In attempts to develop a general new equation, we

*Marangoni number, $Ma = \frac{\partial T}{\partial x} \frac{\partial \sigma}{\partial T} \frac{a^2}{\eta \alpha}$, where $\alpha = k/\rho C_p$ is the thermal diffusivity.

decided to make a few more computer runs for different conditions. Unfortunately Milito's computer program would no longer produce sensible results. Milito has left Clarkson (without the M.S.) and consequently we now have little confidence in his results.

Fortunately Professor Subramanian was able to reach an analytical solution of this problem using a matched asymptotic expansion.[21] The final result is

$$V = \frac{\partial T}{\partial x}\frac{\partial \sigma}{\partial T}\frac{a}{\eta}\left[\frac{1}{2} - \frac{301}{14{,}400}\,Ma^2 + O(Ma^4) - \cdots\right] \qquad (2)$$

which is probably valid roughly up to Marangoni number Ma ~ 1. Note that the first term (1/2) is YGB's result and that only even powered terms in Ma appear. While this result should be sufficient for nearly all glass processing experiments, there are some fascinating mathematical questions in going to high Ma that should be considered in the work.

5.2 Single Bubble Near Surface

In real glass fining (bubble removal) isolated bubbles do not occur in unbounded melts under static conditions. Bubbles interact with one another and with walls. This was certainly true in our SPAR experiment. Thus we have devoted considerable attention to interaction phenomena.

We have solved the problem of a bubble moving near a surface with a temperature gradient normal to the surface.[22] It was found that the bubble slows down from the YGB velocity as it approaches a surface. The retardation begins when the bubble surface is about one diameter from the surface, with the retardation greater for a solid surface than for a free surface (liquid-gas). This may be compared with the larger retardations experienced out to 5 diameters by a bubble rising due solely to buoyancy (gravity).

5.3 Two Bubbles in Large Melt

Meyyappan and Subramanian have also solved the double-bubble problem, using an analytical technique with bispherical coordinates. Since they are still

interpreting these results, a manuscript has not yet been written. They considered two bubbles in line along the temperature gradient. The results are summarized in Figures 5.3-1 and 5.3-2. Note that a small bubble may be greatly accelerated by the presence of a large bubble, with the velocity increasing as the large bubble increases in size and as the distance between the bubbles decreases. The result is the same whether the large bubble is "in front" or the small bubble is in front. The large bubble is slowed down, but only slightly. Bubbles which are both of the same size move at their YGB velocity, i.e. they have no net influence on the movement of one another.

It appears that the large bubble will catch a small bubble when the small bubble is in front, but not vice versa. We are not entirely certain about this, however, because our solution does not yield results when the bubbles are near one another.

5.4 Theoretical Work Remaining

Not all theoretical problems relevent to glass fining have been solved. Among those remaining are:

a. Single bubble at large Marangoni number.
b. Bubble near surface with temperature gradient at angle to surface.
c. Physical explanation for absence of net effect with two bubbles of same size.
d. Two bubbles near one another.
e. Coalescence of two bubbles.
f. Two bubbles not aligned with temperature gradient.
g. Multiple bubbles.

Some of these are probably amenable to analytical approaches, while the solution of others will require numerical modelling on the computer.

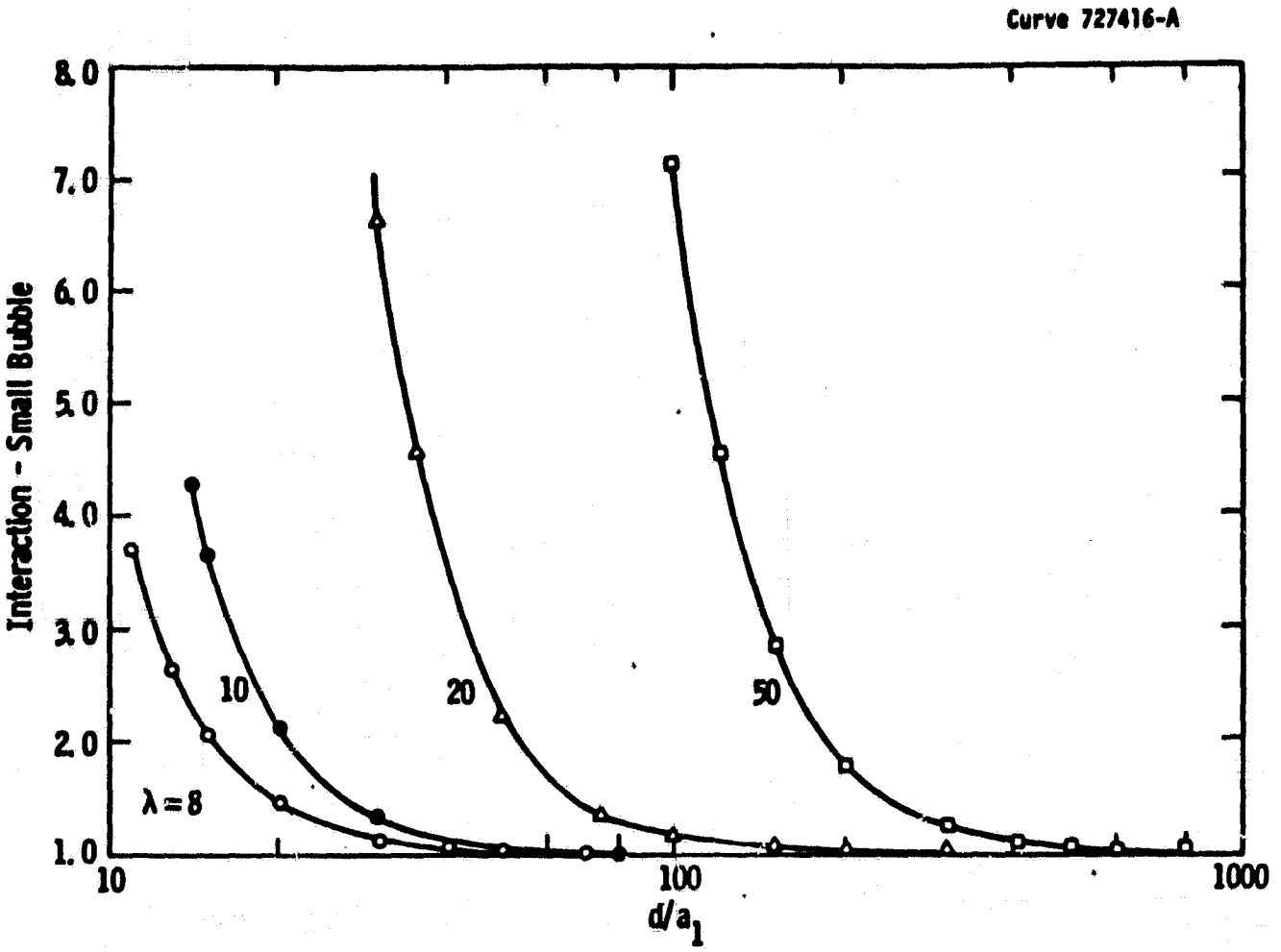

Fig. 5.3-1-Solution to double bubble problem. Here $\lambda = a_2/a_1$, a_2 is the radius of the large bubble, a_1 is the radius of the small bubble, d is the distance between the centers of the bubbles (they touch at $d = a_1 + a_2$), and "INTERACTION" is the ratio of the actual velocity of the small bubble to its YGB velocity

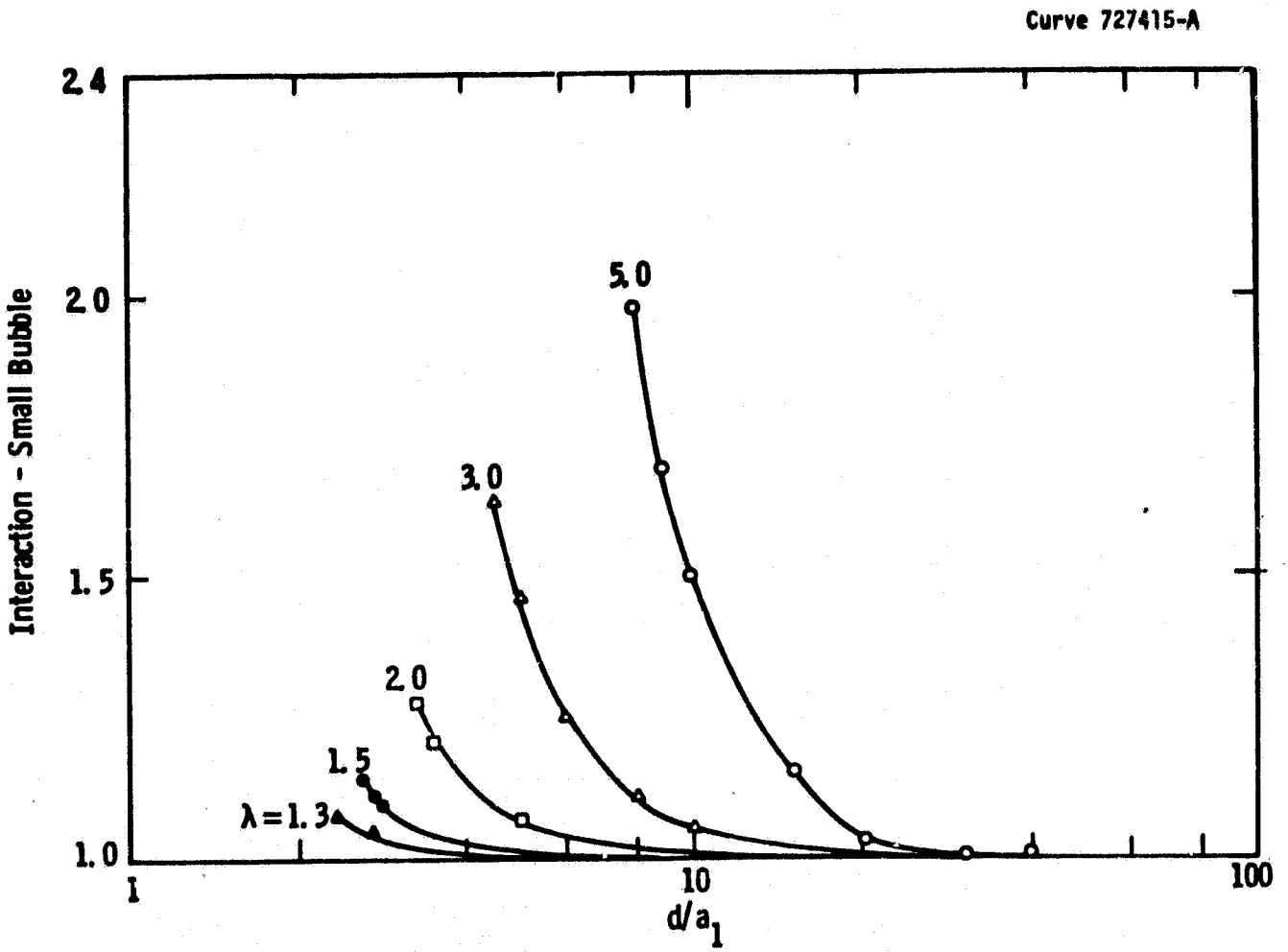

Fig. 5.3-2 —Continuation of figure 5.1 for smaller values of λ (radius ratio)

6. The SPAR VIII Experiment 77-13

Description and Interpretation

6.1 Introduction

On November 18, 1980, the SPAR VIII rocket carrying experiment 77-13 was launched. During the flight, the experimental apparatus operated flawlessly for more than 4 minutes under an average acceleration near zero. During that time, 246 photographs of the molten glass sample were taken at one second intervals. One of these photographs clearly showing abundant bubbles is reproduced in Figure 6.1-1. At the same time, temperature data from the three thermocouples embedded in the molten glass and welded to the heating strip were telemetered back to the ground. Telemetry of a signal proportional to the current drawn by the camera film advance motor provided a time indicator for the film sequence.

The flight film was recovered intact despite a hard landing by the payload. The developed film showed that the bubbles in the molten glass clearly moved toward the hotter areas in the sample. In the following sections we present an evaluation of the experiment performance and a preliminary analysis of the data and a comparison to the theory presented in the previous section.

6.2 Sample Description

The sample was constructed as illustrated in Figures 3.2-2, 4.3-2. Its appearance was changed little by the experiment. The sample without the upper heat shield is shown in Figure 6.2-1a, b, and c. The sample does not appear clear because of the large amount of crazing (cracking) that occurred due to expansion mismatch between the silica and the sodium borate glass when the glass froze. The large void coincident with one of the thermocouple wells at the center of the channel formed during manufacture of the flight sample. The side view shows that the platinum heating strip did not pull away from the

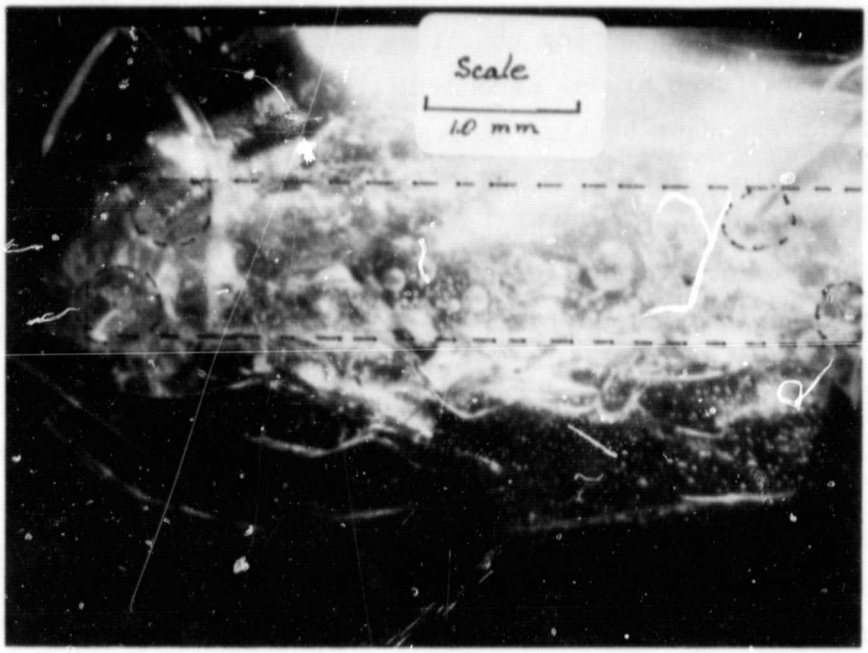

Figure 6.1-1 - Reproduction of one of the 70 mm photographs taken during the flight while the glass sample was molten. Unavoidable crazing (cracking) of the fused silica at the channel walls is visible. Dashed lines indicate the position of the walls and thermocouple lead wells.

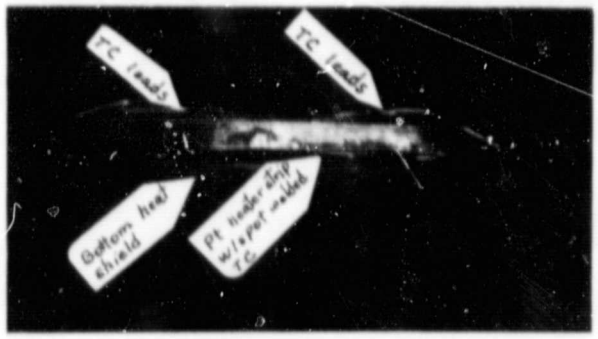

a) Side view of the flight sample (3.3X)

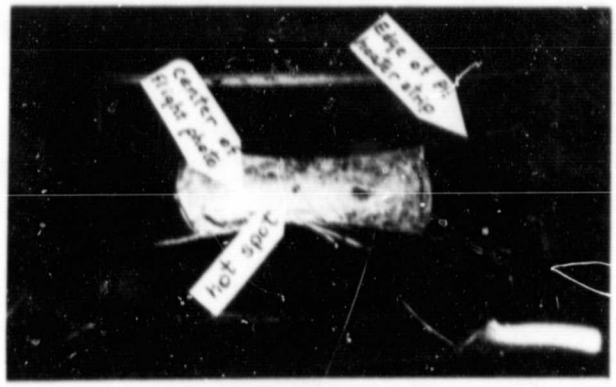

b) Top view of the flight sample (3.3X)

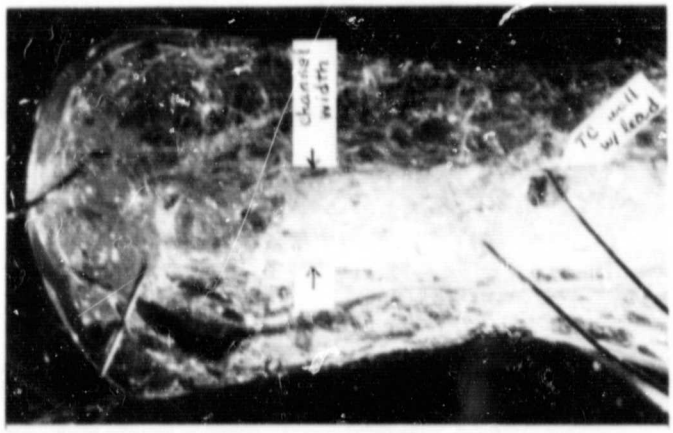

c) Close-up of the photographed area of the flight sample (13.5X)

Figure 6.2-1 - The flight sample with the upper heat shield removed

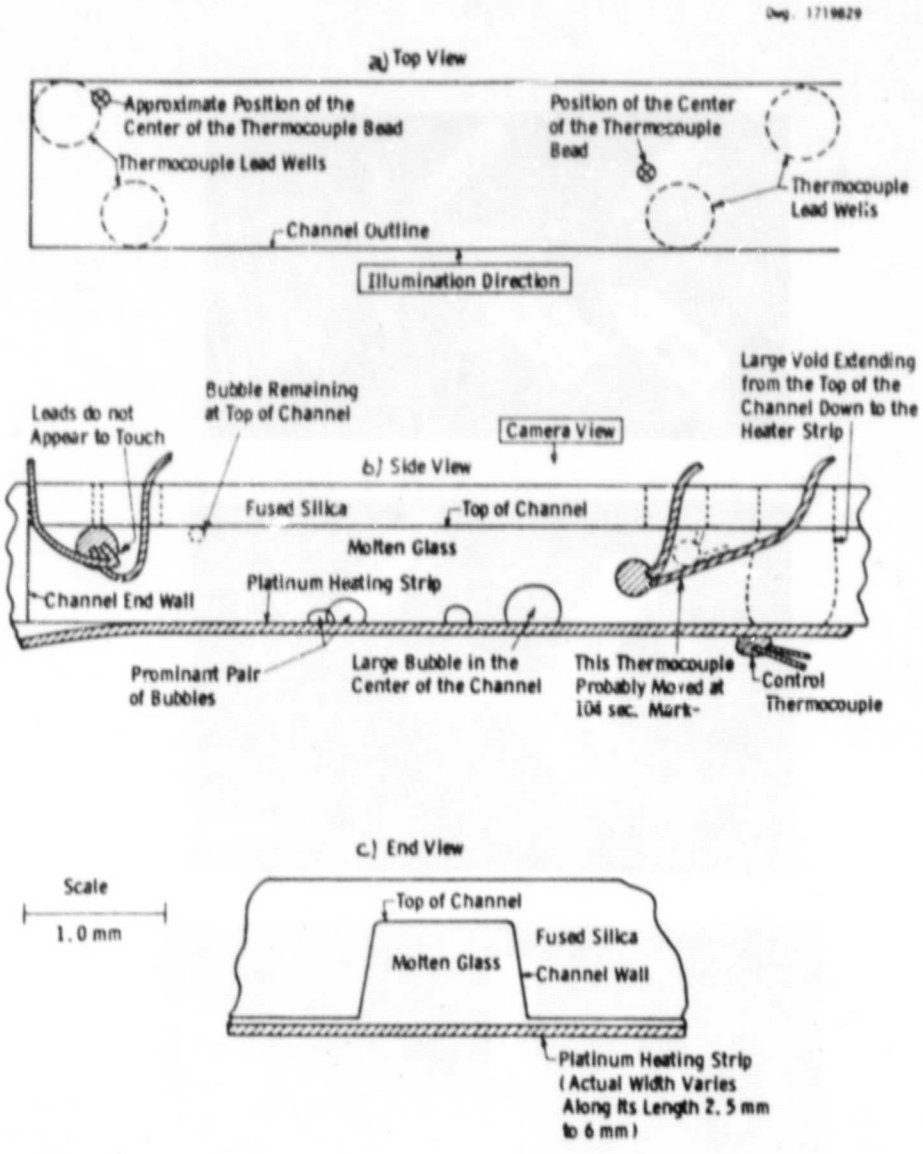

Figure 6.2-2a,b,c - Diagramatic reproduction of photographed section of SPAR Experiment Cell 77-13 and some bubbles. The prominant pair of bubbles is visible in figures 6.1,6.2-3,6.2-4.

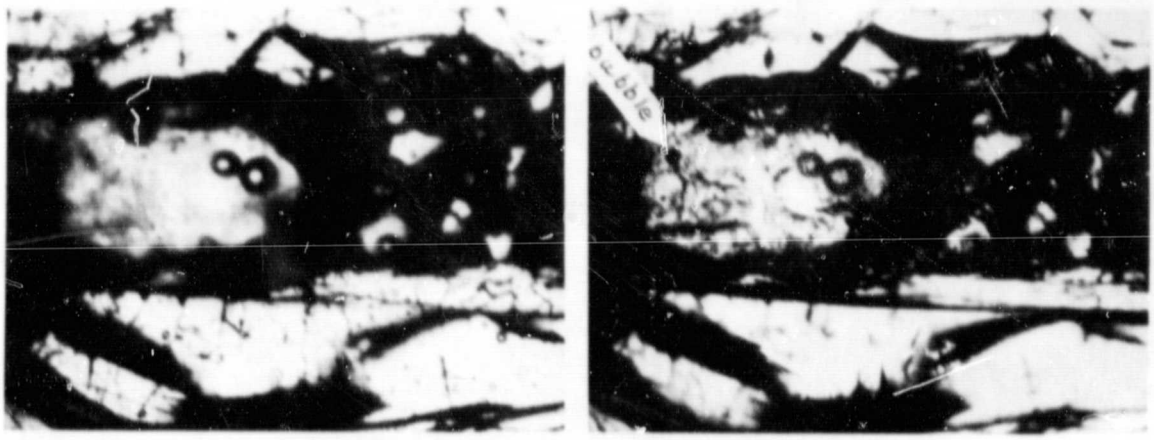

a) focused at the bottom of the channel

b) focused at the top of the channel

Figure 6.2-3 - Top views of the documented region of the flight sample. Bubbles were found to be either at the silica cover or at the platinum heater strip. Transmitted light, 27.5X.

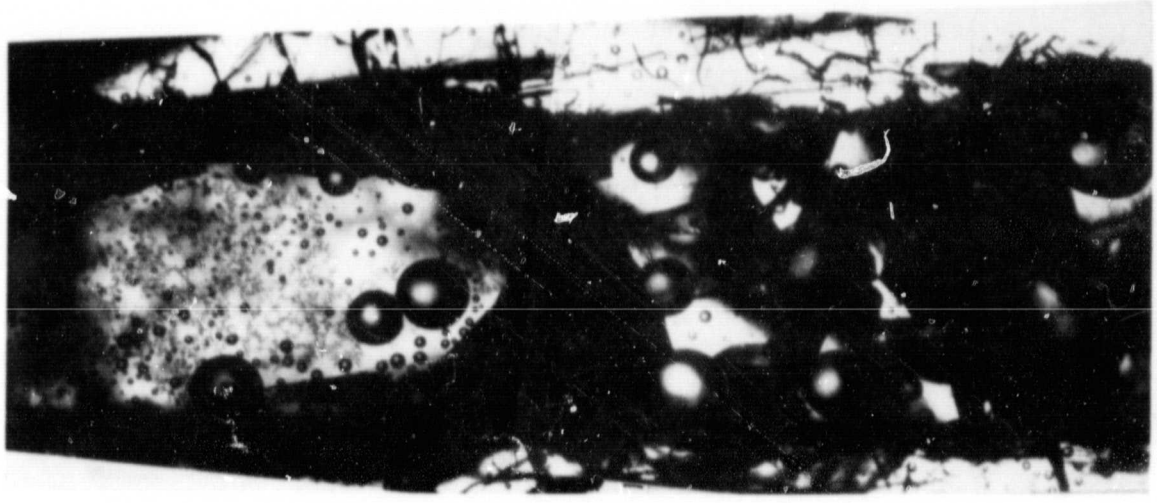

Figure 6.2-4 - Bottom view of documented area of the flight sample. Objective focused on the surface that was next to the heater strip. Almost all of the bubbles were found at this surface. Transmitted light, 44X. Dendritic pattern on the surface is believed to be due to reaction of moisture with the glass after the flight.

silica plate during the flight (Figure 6.2-1b). Figure 6.2-1c shows the area photographed during the experiment. The glass was much clearer during the experiment when it was molten, with the only cracks remaining being those in the silica.

Figure 6.2-2a, b, c is a diagramatic sketch of the flight cell shown in Figure 6.2-1c. The location of the thermocouples was determined by first sectioning the sample alongside each pair of wells and then viewing with the aid of an index oil from both the side and the bottom (after the heater strip was removed). The relative thickness of glass and fused silica as well as the shape of the channel cross section was determined from the sawed sample cross section.

In Figure 6.2-3a, b, the sample is viewed from the top after removing the bottom heat shield and the platinum heater strip. Bubbles were found to be either at the top of the channel (Fig. 6.2-3b) or at the bottom (Fig. 6.2-3a). The objective lens used to make these observations had a focal depth much less than the depth of the channel. By focusing up and down it was apparent that the intervening glass had at least no large bubbles $\gtrsim$30 μm remaining in it. By turning the sample over it was possible to focus directly on the bottom without interference as shown in Figure 6.2-4. The sharpness of all these bubble images indicates that they lay in the focal plane of the objective, and therefore were on the platinum strip. This again reinforces the opinion that all of the bubbles in the flight sample had moved to the platinum strip except for a few which adhered to the silica cover.

6.3 Time-Temperature Data

Temperatures were measured at three different positions in the experiment (see figure 6.2-2). Table I summarizes the available data for the temperatures read by each thermocouple at 10 second intervals. These data were originally taken from the strip chart recording of the telemetry signals made at the time of the flight. These have since been corrected slightly by comparing them to the digitized telemetry data provided by Marshall Space Flight Center. Corrections were 5°C or less.

Table 1 - Time-Temperature Telemetry Data

Time (from lift-off)	Control TC (on heater strip)	TC in Glass (hot spot)	TC in Glass (cooler and sample)
94 (sec.)	ambient	ambient	ambient
104	833°C	675°C	432°C
114	908	838	562
124	911	851	600
134	911	859	628
144	912	862	647
154	912	867	659
164	912	869	669
174	912	872	676
184	912	872	682
194	912	873	688
204	913	873	691
214	913	874	694
224	913	874	696
234	913	874	697
244	913	874	698
254	913	875	700
264	913	875	701
274	913	875	701
284	913	875	701
294	913	875	703
304	913	875	703
314	913	875	703
324	913	875	703
334	913	875	703

The temperatures approached steady state asymptotically. The farther a thermocouple was from the heating area the longer it took to come to equilibrium. This is one reason we made the system so small. It is clear that any bubble motion studies made roughly during the first 120 seconds will have to consider the changing temperature and temperature gradients. After about 120 seconds the temperature changes were small and so probably insignificant in comparison with the perturbing effects of bubble interactions and proximity to silica or platinum surfaces. Note that since velocity is proportional to ∇T, we need only to know the parallel gradient because we are measuring velocity in that direction.

Figure 6.3-1 is a diagram taken from Figure 6.2-2 with a preliminary estimate of the attitude of the isothermal surfaces in the flight sample. It is clear that the thermocapillary force was directed toward the hot spot on the platinum strip with components of the force both parallel and perpendicular to the strip. The attitude of the isotherm at the hot spot was estimated by assuming that the temperature gradient perpendicular to the heater strip was the same as the gradient between the control thermocouple on the strip and the thermocouple in the glass. This estimate is consistent with previous laboratory measurements of this gradient. The other isotherms are considered to be parallel to that one. The trajectories of the bubbles should be perpendicular to the isotherms, except when they are near other bubbles or near the platinum or silica surfaces.

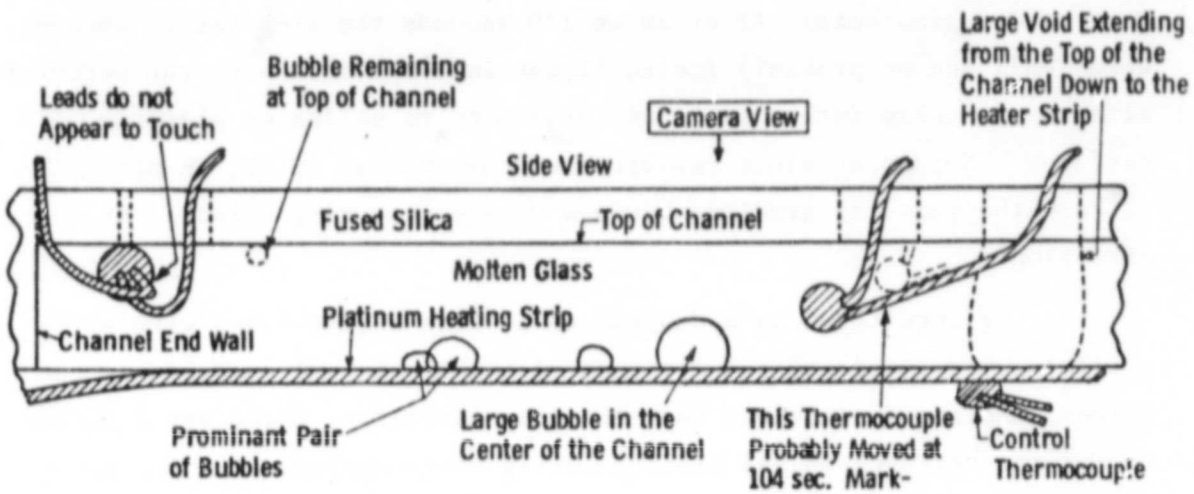

6.3-1 - Some postulated isotherms superimposed on Figure 6.2-2b.

6.4 A Preliminary Analysis of Bubble Motion in the Presence of a Temperature Gradient Under Zero Gravity Conditions

Since the flight film from experiment 77-13 was developed and subsequently made into a strip of 16 mm movie film, we have had the opportunity to observe the motion of the bubbles repeatedly. Based on these observations and the post flight evaluation of the flight sample, we have been able to qualitatively analyze the bubble motion that occurred during the SPAR VIII flight. Unfortunately it took much longer than anticipated to reproduce the same film strip on the stock that is appropriate for the Clarkson Vanguard Motion Analyzer, so Mr. Meyyappan of Clarkson has had a minimal amount of time to make quantitative measurements of bubble motion and even less time to make a careful comparison with the theory. This analysis is continuing and a thorough analysis of the film and comparison of the bubble motion with theory will be forthcoming.

We will restrict our analysis here to general observations and to a first order evaluation of the motion of the few bubbles that Mr. Meyyappan has been able to track with the motion analyzer.

6.4.1 Comments About the Film

The strip of movie film was made by copying the flight film frame for frame. The movie film differs from the flight film in that only the center half of the flight film was copied. This was done because the Nikon was set to take a double 35 mm frame (i.e. 70 mm) which gave excellent coverage of the experiment but could not be directly reproduced in full on the 16 mm frame. However the section reproduced was selected after studying the flight film. It appears to contain the most pertinent information.

6.4.2 Data Analysis Using Vanguard Motion Analyzer

The procedure involved the tracking of the center of a given bubble through the frames, i.e. as a function of time. Usually this was done by placing the vertical and horizontal cross wires of the analyzer tangential to the bubble at points 1, 2, 3, and 4 successively. The corresponding x and y coordinate values and frame number (and hence

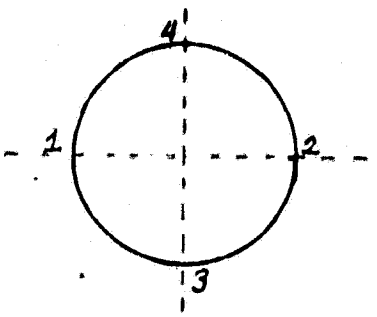

the time) may be fed directly to an IMSAI 8080 computer wherein these data are stored on disks. A basic program to manipulate this data to obtain the necessary parameters is available. Unfortunately the IMSAI was malfunctioning, and so all data taking and analysis were done manually because of the short time available.

In observing the SPAR film it was noted that the frames jumped around a bit. (This also occurred in the Papazian Grumman films). In order to ascertain the correct bubble motion it was therefore also necessary to measure the position of an immobile reference (fiducial) mark. A crack was selected which seemed to be stationary.

A few observations are worth mentioning.

1. The time duration of the experiment was 240 secs (and hence 240 frames). However the first 110 or 120 frames contain little useful data because during this period the temperature profile was being established. With melting in progress, some bulk melt movement may have occurred. After 120 seconds the temperature readings were steady.

2. This analysis has some level of uncertainty (i.e. in data measurement), which is yet to be determined. Repeat measurements at a later date will establish this.

3. The size of each bubble was also calculated from the measurements. This did change during the course of the experiment. Some fluctuations were probably the consequence of measurement errors, especially since the bubbles were not as clear in some frames as in others. Expansion of the bubbles due to changes in temperature and coalescence also occurred as they moved toward the hot end of the channel. Coalescence with a neighboring small bubble was observed with one bubble that was monitored.

6.4.3 General Observations

The experiment can be broken down into two general periods of activity. The first period is the melt-down of the glass. During this period the sample becomes much more transparent as the fractures disappear in the melting glass. As the clearing proceeds, many bubbles are observed moving toward the hot spot. However since this is a period of rapid temperature change and melting, it is impossible to know how much of the bubble motion is thermocapillary migration and how much is mechanical re-equilibration. Certainly there is some of both. The second period is perhaps twice as long as the first. It is characterized by the motion of one or two bubbles at a time while the others (there are many visible) seem to be stationary. Those that move seem to accelerate during their movement and then come to a sudden stop. Some bubble coalescence is observed.

Based on what is known about the orientation of the temperature gradients in the channel and what can be observed in the film, the following general explanation can be given for the observed motion. Many of the bubbles initially formed in the glass as it melts are rapidly swept out of the glass by the high temperature gradients that are present while the sample is heating up. Since there is also a strong vertical gradient these bubbles not only migrate along the channel but vertically to the platinum heater strip. Once they contact the strip they

become attached to it, and move only slowly at best. As the experiment progresses bubbles that were in cooler areas and/or at the top of the channel are slowly drawn toward the center of the channel. Bubbles touching the top of the channel may tend to stick there.

6.4.4 Measurement and Evaluation of the Motion of Three Bubbles

Two prominent bubbles in the center of the channel were observed to execute the motion shown in Figures 6.4-1 and 6.4-2. For convenience the bubble positions were plotted in cm as viewed on the motion analyzer vs. time. The magnification factor has since been determined to be 42.7 ± 1. (These bubbles are clearly visible in Figure 6.1-1 near the center. The larger of the pair is 212 μm in diameter; the smaller, 165 μm). Bubble 1 begins to move slowly, then accelerates and finally comes to a sudden stop. Bubble 2 appears to behave in a similar way, as again it appears to be accelerating when it suddenly comes to almost a complete stop. The early motion of bubble #2 was partially obscured by a small crack in the silica at the top of the channel. Therefore bubble #2 was not tracked in the earlier part of the motion, but its behavior appears to be similar to that of bubble #1.

The motion of these two bubbles appears to be consistent with the general picture outlined in the preceding section. These bubbles appear to have been in contact with the top of the channel, moving at first very slowly, perhaps retarded by interaction with the wall. Finally as they move away from the wall, the influence of the temperature gradient takes over and the bubble moves horizontally toward the hot spot on the heater strip and at the same time downward toward the strip because of the vertical temperature gradient. The bubble accelerates as its diameter increases and as the melt viscosity decreases with increasing temperature. Note that the temperature coefficient of surface tension is quite constant over the range of temperatures encountered. Therefore, the observed change in bubble velocity is most likely due to the above reasons. When the bubble strikes the heater strip it apparently sticks quite strongly judging from its lack of movement after that instant.

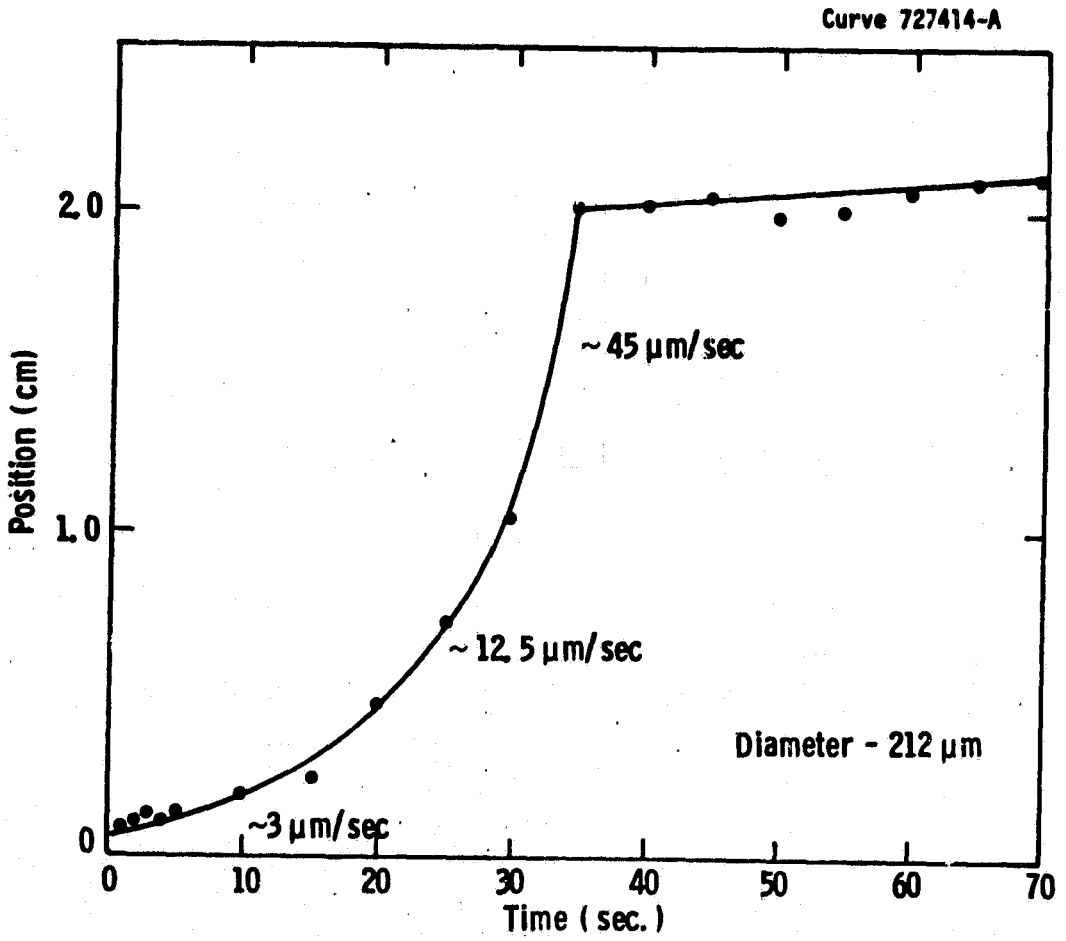

Fig. 6.4-1—Bubble #1

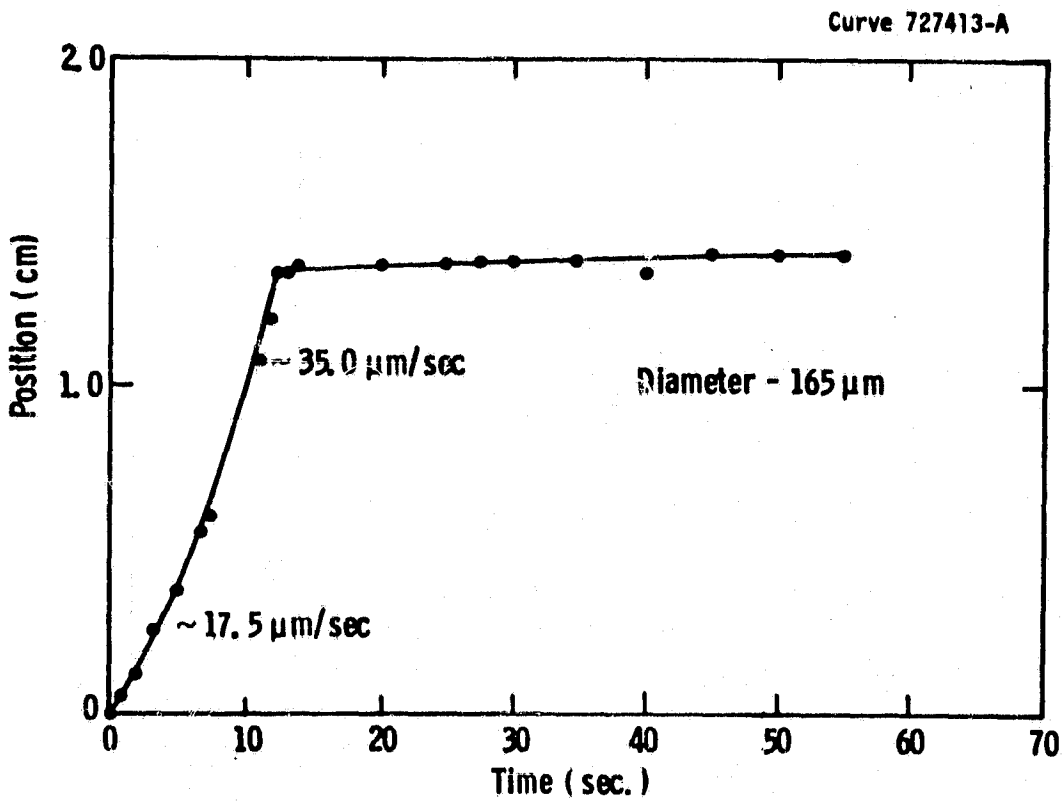

Fig. 6.4-2--Bubble #2

The velocities indicated on Figures 6.4-1 and 6.4-2 are the horizontal components of the actual bubble velocities, but they should be directly proportional to the actual velocities. Since the horizontal temperature gradient is measured during the experiment we can make a zero-order comparison with the modfied YGB theory from Chapter 5. According to the YGB theory, the velocity of the bubble v is

$$v = \left|\frac{\partial T}{\partial X}\right| \left|\frac{\partial \gamma}{\partial T}\right| \frac{a}{2\eta}$$

where $\frac{\partial T}{\partial X}$ = 438 °C/cm (from the temperature table)

$\frac{\partial \gamma}{\partial T}$ = .0756 dyne/cm °C[14]

η = the viscosity in poise

a = the bubble diameter, .0212 cm, .0165 cm

The horizontal YGB velocities are 35 μm/sec for bubble 1 and 27 μm/sec for bubble 2. These velocities are in the same ratio as those estimated in Figures 6.4-1 and 6.4-2 for the rapid period of motion (i.e. 45 and 35 μm/sec). This strongly indicates that the velocity of the bubble is linearly dependent on its diameter, as predicted by the theory. The YGB velocties were calculated assuming a viscosity of 100 poise which is a reasonable value in the estimated temperature range of 750°-800°C. Clarkson is currently conducting a more thorough analysis of the bubble motion and its relation to the thermal field. When this is complete, it will be possible to make a more precise comparison between the theory and experiment. Though a complete verification of the theory cannot be conducted, there are no serious discrepancies.

Bubble 3 is an example of a bubble "stuck" to the platinum heater strip. Figure 6.4-3 shows the measurements taken in Bubble 3. Bubble 3 maintained a fairly constant size of about 76 μm diameter. (on the screen). This corresponds to a YGB velocity of 4.9 μm/sec. In Figure 6.4-3 the data are extremely scattered and it appears that

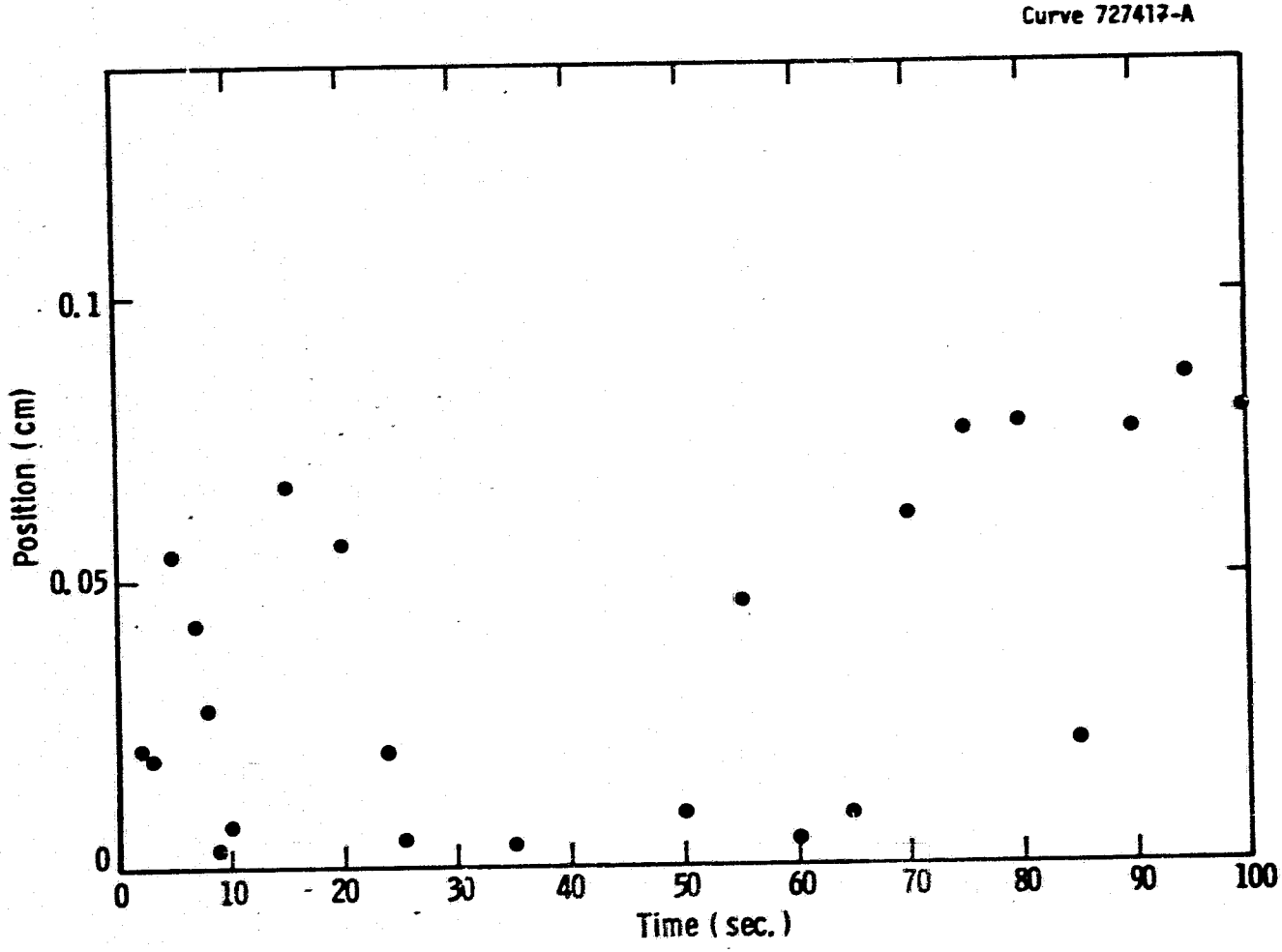

Fig. 6.4-3—Bubble #3

there was vibration or oscillation, but no appreciable net movement. In the neighborhood of Bubble 3, another bubble of roughly the same size was also analyzed. It exhibited a similar oscillatory behavior. We believe these bubbles were "pinned" to the platinum strip and exhibited oscillatory behavior either due to the movement of nearby "free" bubbles, or to an inherent oscillation of the thermocapillary plumes emitted by each. This is an interesting phenomenon not reported previously. In the months ahead we will quantify this behavior in more detail and attempt to determine a mechanism.

6.5 Concluding Comments

It is clear from our work to date that the motion of the bubbles is consistent with the Clarkson model of thermocapillary bubble migration. This conclusion is based on the observed direction and rates of bubble motion and the known orientation of isothermal surfaces in the flight experiment sample. The agreement is at present only semi-quantitative and it will take further careful analysis of the flight data to determine if they will provide a quantitative test for the theoretical model. This analysis is currently under way.

Other new information is also anticipated from further analysis of the data. Our preliminary observations have already shown that bubble coalescence, bubble-bubble interaction, and bubble-wall interaction all occurred during the flight experiment. If even semi-quantitative information can be extracted from the flight data it will indicate the validity of the theoretical models of these kinds of bubble intereactions. Hence we expect to obtain some equally exciting results from this further study of the flight data.

Further studies of the thermocapillary migration need to be carried out under zero gravity conditions. The present experimental system could perform several kinds of additional experiments such as measuring

thermocapillary bubble migration glass systems with different surface tension temperature coefficients (e.g. positive) or melts containing a volatile component (e.g. water in a borate glass). These data, in addition to confirming our SPAR VIII results, will either confirm the general applicability of the Clarkson model or demonstrate its limitations and indicate suitable modifications.

The present system may prove to be too qualitative to provide a proper test for the Clarkson model. In that case, the experimental system should be redesigned probably to a larger size and the definitive experiments run on a shuttle flight. In any case an additional SPAR flight with the present apparatus design is in order, perhaps with borax at a lower temperature so that more bubble-bubble interactings can be observed.

REFERENCES

1. G. E. Rindone, Fining, Part I, Glass Industry, 38 (9) 1957 pg. 489-528.

2. G. E. Rindone, Fining, Part II, Glass Industry, 38 (10) 1957, pg. 561-577.

3. S. R. Scholes, Modern Glass Practice, Cahness Books, Boston, Mass., 1975, pg. 216.

4. C. H. Greene and R. F. Gaffney, Apparatus for Measuring the Rate of Absorption of a Bubble in Glass, J. Am. Ceram. Soc. 42(6) 1959, pg. 273.

5. M. Cable, A. R. Clarke, M. A. Haroon, Glass Tech. 9. (1968) p. 101; 10 (1969) p. 15.

6. L. Nemec, "Refining in the Glass Melting Process," J. Amer. Ceram. Soc., 60, No. 10 436-40 (1977).

7. C. H. Greene and A. Haynes, Jr., Effect of As_2O_3 and $NaNO_3$ on the Solution of O_2 in Soda-Lime Glass, J. Am. Ceram. Soc., 48 (10) 1965 p. 528.

8. N. O. Young, J. S. Goldstein, and M. J. Block, "The Motion of Bubbles in a Vertical Temperature Gradient," J. Fluid Mech. 6, 350 (1959).

9. E. Roedder, 1965 Meeting of the Geological Society of America (from U.S. Geological Survey).

10. W. R. Wilcox, "Anomalous Gas-Liquid Inclusion Movement," Ind. Eng. Chem. 61, 76 (March 1969).

11. T. R. Anthony and H. E. Cline, "The Thermomigration of Biphase Vapor-Liquid Droplets in Solids," Acta. Met. 20, 247 (1972).

12. S. R. Coriell, S. C. Hardy and M. R. Cordes, "Melt Shape in Weightless Crystal Growth," NBSIR 77-1208, Feb. 1977.

13. H. D. Smith, D. M. Mattox, W. R. Wilcox, and R. S. Subramanian, "Glass Fining Experiments in Zero Gravity," Final Rept. to George C. Marshall Space Flight Center, Contract No. NAS8-32351, June 30, 1977.

REFERENCES (Cont'd)

14. Partlow, D. P., H. D. Smith, and D. M. Mattox, "Variation in the Surface Tension of Molten Sodium Borate With Temperature," Phys. Chem. Glasses, Vol. 21, No. 6, 221-224, 1980.

15. Matusita, K., T. Watanabe, K. Kamiya, and S. Sakka, "Viscosities of Single and Mixed Alkali Borate Glasses," Phys. Chem. Glasses, Vol. 21, No. 2, 78-84, 1980.

16. Shartsis, L., W. Capps, and S. Spinner, "Viscosity and Electrical Resistivity of Molten Alkali Borates," Jour. of Am. Cer. Soc., Vol. 36, No. 10, 319-326, 1953.

17. Kaiura, G. H., and J. M. Toguri, "The Viscosity and Structure of Sodium Borate Melts," Phys. Chem. Glasses, Vol. 17, No. 3, 62-69, 1976.

18. S. C. Hardy, "The Motion of Bubbles in a Vertical Temperature Gradient," J. Colloid Interface Sci. 69, 157 (1979).

19. J. L. McGrew, T. L. Rehm and R. G. Griskey, "The Effect of Temperature - Indiced Surface Tension Gradients on Bubble Mechanics," Appl. Sci. Res. 29, 195 (1974).

20. R. L. Thompson, K. J. deWitt, and T. L. Labus, "Marangoni Bubble Motion Phenomenon in Zero Gravity," Chem. Eng. Commun. 5, 299 (1980).

21. Subramanian, R. Shankar, "The Slow Migration of a Gas Bubble in a Thermal Gradient." Accepted for publication, AIChE Journ. Sept. 1980.

22. Meyyappan, M., W. R. Wilcox, and R. Shankar Subramanian, "Thermocapillary Migration of a Bubble Normal to a Plane Surface." Accepted for publication, Journ. of Colloid and Interface Science, Jan. 1981.

ACKNOWLEDGMENTS

This report describes an experiment that was the outcome of a team effort of several of Westinghouse contributors. Their names follow:

R. G. Seidensticker - Hot stage - design and evaluation.

R. A. Johnson - Electronic systems - power supply, control, and telemetry interface.

N. A. Salemi - Flight experiment assembly - integration of hardware and electronic systems.